Antarctic sea ice response to meltwater due to Antarctic ice sheet mass loss in a multi-model ensemble

Andrew G. Pauling[1], Inga J. Smith[1], Torge Martin[2], Jeff K. Ridley[3], David P. Stevens[4,5], Max Thomas[1,3], Rebecca L. Beadling[6], Christopher Danek[7], Tore Hattermann[8], Qian Li[9], John Marshall[9,10], Morven Muilwijk[8], Ariaan Purich[11], and Neil C. Swart[12]

[1]Department of Physics, University of Otago, Dunedin, New Zealand
[2]GEOMAR Helmholtz Centre for Ocean Research Kiel, Kiel, Germany
[3]Hadley Centre, UK Met Office, Exeter, UK
[4]Centre for Ocean and Atmospheric Sciences, University of East Anglia, Norwich, UK
[5]School of Engineering, Mathematics and Physics, University of East Anglia, Norwich, UK
[6]Earth and Environmental Science Department, Temple University, Philadelphia, USA
[7]Alfred Wegener Institute for Polar and Marine Research
[8]Norwegian Polar Institute, Fram Centre, Tromsø, Norway
[9]Department of Earth, Atmospheric, and Planetary Sciences, Massachusetts Institute of Technology, Cambridge, MA, USA
[10]NASA Goddard Institute for Space Studies, New York, NY, USA
[11]School of Earth, Atmosphere and Environment and and ARC Special Research Initiative for Securing Antarctica's Environmental Future, Monash University, Clayton, Kulin Nations, Australia
[12]Canadian Centre for Climate Modelling and Analysis, Environment and Climate Change Canada, Victoria, BC, Canada

Correspondence: Andrew G. Pauling (andrew.pauling@otago.ac.nz)

Abstract. We present the first multi-model study of the Antarctic sea ice response to enhanced meltwater due to dynamic mass loss from the Antarctic ice sheet. This meltwater flux (and its future increase under global warming) is not included in the most recent state-of-the-art climate model simulations used in CMIP6, representing a missing source of freshwater to the Southern Ocean. Previous climate model simulations have shown a wide range of responses in Antarctic sea ice and climate when this missing meltwater is introduced. Here, we analyze a new suite of 11 models comprising 43 ensemble members to assess the response to 0.1 Sv of Antarctic meltwater input at the ocean surface, evenly distributed around the Antarctic coastline under pre-industrial control forcing. Antarctic sea ice area increases in all models. However, there is a wide range in the response, with annual mean increases ranging from 0.71 to 4.14 million km^2. There is also substantial variation in both the spatial distribution and the time scale of the sea ice response. The intermodel spread in sea ice response is influenced by the model mean-state sea ice area and volume, the prevalence of open-ocean deep convection, and the mean-state stratification of the ocean. These findings highlight the importance of model mean-state biases in determining the response to a missing Antarctic meltwater boundary condition.

1 Introduction

The evolution of the extent of Antarctic sea ice during the satellite era has differed substantially from that in the Arctic. Antarctic sea ice area has increased slightly over time, reaching a record high in 2014, before experiencing a rapid decline since

that time (Parkinson, 2019; Roach and Meier, 2024). In contrast, the Arctic sea ice has declined relatively steadily (Stroeve and Notz, 2018). State-of-the-art climate models, such as those participating in phase 6 of the Coupled Model Intercomparison Project (CMIP6, Eyring et al., 2016) have generally failed to reproduce the observed trends in Antarctic sea ice (Roach et al., 2020), and most models simulate a fairly steady decline.

One proposed reason for the discrepancy between modeled and observed sea ice trends is the inability of most climate models to account for increasing meltwater from the Antarctic ice sheet. Freshwater input to the Southern Ocean, resulting from the melting of the Antarctic ice sheet and ice shelves, has been increasing throughout the satellite era. Slater et al. (2021) reviewed Earth's ice mass imbalance and estimated that the mass loss from the Antarctic ice sheet and ice shelves was 395 ± 99 Gt yr^{-1} during the period 1994-2017, and 509 ± 186 Gt yr^{-1} over the period 2010-2016. In general, climate models lack an Antarctic ice sheet that interacts with the atmosphere and ocean, and thus cannot realistically represent the mass imbalance for the ice sheet. For example, in many models, including all the models participating in CMIP6 (Siahaan et al., 2022), ice sheet mass balance is enforced, meaning that the rate of freshwater input to the Southern Ocean from the Antarctic ice sheet can only change in step with the amount of precipitation falling on the Antarctic continent. In the real world, ice sheet mass balance is determined by the input from precipitation over the continent and ice loss at the coast via processes such as basal melting and iceberg calving. In light of the urgency of understanding this system, in lieu of the substantial model development effort and computational expense required to implement coupled ice sheets in climate models, many studies have instead conducted simulations with artificially increased freshwater input to the Southern Ocean from the continent (see Table 1 in Swart et al., 2023). Including this missing source of freshwater in coupled model simulations has been shown to improve the model representation of the sea surface temperature (SST) of the Southern Ocean and the trends of sea ice (Schmidt et al., 2023; Roach et al., 2023; Kaufman et al., 2025). Anomalous meltwater input to the Southern Ocean has also been shown to have remote impacts in the tropics through atmospheric teleconnections (Dong et al., 2022a, b; Beadling et al., 2024; Xu et al., 2025) and impacts on precipitation (Bronselaer et al., 2018). Consequently, it has been proposed that anomalous meltwater should be included as a standard forcing in future phases of the Coupled Model Intercomparison Project (Schmidt et al., 2023).

Several previous studies that focused on explaining the discrepancy between modelled and observed Antarctic sea ice trends have highlighted the potential role of additional Antarctic meltwater. These studies hypothesize that the increased ocean stratification due to the additional meltwater inhibits vertical transport of relatively warm water from depth to the surface around Antarctica, resulting in increased sea ice formation. For example, Bintanja et al. (2013) and Bintanja et al. (2015) reported that 120 Gt yr^{-1} of additional freshwater was sufficient to reverse the modeled decline in Antarctic sea ice extent in the EC-Earth climate model. Swart and Fyfe (2013) used the UVic climate model with various rates of linear increase in freshwater input into the Southern Ocean. In their most extreme scenario, the freshwater input increased from 0 to 883 Gt yr^{-1} over 28 years. In contrast to Bintanja et al. (2013) and Bintanja et al. (2015), Swart and Fyfe (2013) reported that this additional freshwater was not sufficient to compensate for the modeled decline in the Antarctic sea ice area. Pauling et al. (2016) used the Community Earth System Model version 1 (CESM1) with various rates of freshwater input, either at the ocean surface or at the depth of the ice shelf fronts around Antarctica, concluding that a constant freshwater input of up to 3000 Gt yr^{-1} was insufficient to reverse the trend in the Antarctic sea ice area. In addition, Pauling et al. (2016) found that the increase in net precipitation over the

Southern Ocean between the preindustrial and present day is about 2500 Gt yr^{-1} in CMIP5 models, a freshwater source that is an order of magnitude larger than the input rates used by the two studies by Bintanja et al. mentioned above. In a subsequent study, Pauling et al. (2017) introduced a linear increase in freshwater input in CESM1, with rates increasing from 0 to 4000 Gt yr^{-1} over a 34-year period. Building on previous work (Swingedouw et al., 2008; Hattermann and Levermann, 2010; Wang and Beckmann, 2007) they also tested the sensitivity to including the effect of removing the latent heat required to melt the ice from the ocean. Although the very high meltwater input rates in Pauling et al. (2017) were able to reverse the modeled trend in the Antarctic sea ice area, they are much larger than recent estimates of the Antarctic Ice Sheet mass imbalance (Slater et al., 2021).

The impacts of meltwater due to Antarctic mass loss on other aspects of the climate system have also been studied in fully-coupled climate models. Gorte et al. (2023) found that the projected meltwater from Antarctica over the 21st century results in a 72% decrease in the deep convective area of the Southern Ocean during winter and 83% more Antarctic sea ice relative to projections that do not include the meltwater. Bronselaer et al. (2018) used the GFDL-ESM2M model with 10 ensemble members to investigate the response of the climate system to Antarctic meltwater under a future high-emission and high-meltwater scenario. They found that the meltwater was able to drive an increase in Antarctic sea ice area until about 2060, after which the warming due to increased greenhouse gas concentrations dominates and sea ice area declines again. With a similar high meltwater forcing, simulations with the ACCESS-ESM1.5 model found that meltwater drives an increase in Antarctic sea ice until 2030, with greenhouse forcing dominating thereafter (Purich and England, 2023). Both Bronselaer et al. (2018) and Purich and England (2023) also found that the meltwater induced a northward shift of the intertropical convergence zone (ITCZ), highlighting the global implications of including this missing process in climate models.

Although the impact of Antarctic meltwater on sea ice has been extensively studied, the sea ice response appears to be highly model dependent. Assessing the reasons for this model dependence and quantifying the associated uncertainty has proved difficult due to differences in the model configurations and both the meltwater and the climate scenario applied. This difficulty was a leading motivation for the creation of the Southern Ocean Freshwater Input from Antarctica (SOFIA) initiative (Swart et al., 2023), which defines a series of model experiments to be run by various coupled climate models worldwide, facilitating an intermodel comparison through a standardized experimental design. The SOFIA initiative has also been approved as a CMIP7-endorsed model intercomparison project.

In this study, we present results from the “Tier 1" *antwater* SOFIA experiment, where a constant 0.1 Sv (3154 Gt yr^{-1}) meltwater perturbation is evenly distributed at the ocean surface evenly across all grid cells immediately adjacent to the Antarctic coastline, under pre-industrial climate conditions. Although this amount of meltwater is larger than contemporary observational estimates of ice shelf basal melt rates (0.035–0.050 Sv, Adusumilli et al., 2020; Davison et al., 2023) or Antarctica’s current mass imbalance (0.006–0.016 Sv, Slater et al., 2021), the *antwater* experiment was designed to produce a robust signal for the purposes of model intercomparison, not to match observations over the historical period. This magnitude of meltwater input is comparable to the projected meltwater flux in the mid to late 21st century (e.g., Swart et al., 2023). The idealized nature of the *antwater* experiment allows us to examine the response to an increase in Antarctic meltwater without the additional interaction

Table 1. Participating models in the SOFIA project used in this study.

Model	Resolution (ocn/atm, lat×lon, °)	Ensemble Members	Freezing Point	Reference
ACCESS-ESM1-5	1/1.875×1.25	5	Linear	Ziehn et al. (2020)
AWI-ESM-1-REcoM	0.69[a]×0.89[a]/1.875×1.875	1	Constant	Semmler et al. (2020)
CanESM5	1/3	10	Non-linear	Swart et al. (2019)
CESM2	1/ 0.9x1.25	3	Non-linear	Danabasoglu et al. (2020)
EC-Earth3	1/1	4	Non-linear	Döscher et al. (2022)
FOCI	0.5/1.9	8	Non-linear	Matthes et al. (2020)
GFDL-CM4	0.25/1	1	Linear	Held et al. (2019)
GFDL-ESM4	0.50/1	1	Linear	Dunne et al. (2020)
GISS-E2-1-G	1×1.25/2×2.5	5	Non-linear	Kelley et al. (2020)
HadGEM3-GC3.1-LL	1/1.875×1.25	4	Non-linear	Kuhlbrodt et al. (2018)
NorESM2-MM	1/1	1	Non-linear	Seland et al. (2020)

[a] Global average of unstructured horizontal resolution.

with anthropogenic greenhouse gas or aerosol forcing. We use this multi-model ensemble to investigate the factors contributing to the inter-model spread in the response of Antarctic sea ice and the Southern Ocean to meltwater input.

2 Data and Methods

Table 1 lists the models that participated in the *antwater* experiment outlined in the SOFIA experimental design. For models that ran more than one ensemble member, we computed the results as the ensemble mean to reduce the impact of internal variability. For SOFIA, the protocol requested that the ensembles be generated by branching each member from a different year in the model's CMIP6 *piControl* run, where the years are chosen to have different phasing of low-frequency ocean variability. Thus, when computing the response for a given variable, each ensemble member is compared with the corresponding time period of the model's CMIP6 *piControl* run. The time averages of the response are always based on the last 30 years of monthly-mean output of the 100-year-long experiment, if not stated otherwise. Statistical significance of the anomalies was computed using a 2-tailed Student's t-test. A potentially important consideration in how each model responds to the addition of meltwater is how the ocean model computes the freezing point of seawater. Thus, in Table 1 we note whether the model uses a constant freezing point of seawater, or a linear or non-linear relationship between the salinity and the freezing point of seawater.

As a point of reference we include satellite observations of Antarctic sea ice area (Fetterer et al., 2025) when analyzing the sea ice area mean state across models. While the *antwater* simulations are under pre-industrial control forcing, and so the sea ice mean state should not necessarily be close to present day conditions, we include the observations to show how far from modern conditions each model may or may not be.

To quantify the effect of additional meltwater on the stratification of the Southern Ocean, we make use of a modified version of the stratification index (SI), as used in Sgubin et al. (2017), Bourgeois et al. (2022) and Weiffenbach et al. (2024). This is typically defined as the sum of the difference in potential density referenced to 0 dbar between each depth and the surface in 200 m depth increments down to 2000 m depth. Here, we modify the definition to sum the density in 50 m depth increments down to 500 m depth (after linear interpolation of the density to these depth levels) in order to better capture the stratification around the mixed layer, where we expect the addition of Antarctic meltwater to have the largest effect on sea ice:

$$SI = \sum_{i=1}^{10} \rho(z_i) - \rho(z_0), \tag{1}$$

where z_0 is the ocean surface and $z_i = z_{i-1} + 50$ m for $i = 1, ..., 10$ (units of z in meters).

We computed the deep mixed volume (DMV) as a metric for the amount of open-ocean deep convection that occurs in the Southern Ocean in each model. Following the method of Chen et al. (2023), DMV is calculated by finding all grid cells south of 55°S with a monthly-mean mixed-layer depth (MLD) greater than 2000 m, multiplying the MLD by the area of the grid cell and adding all grid cells. We used the CMIP6 variable “mlotst" for the mixed-layer depth, which is calculated on the model's timestep, and when computing the annual mean, we compute the monthly DMV before taking the annual mean, rather than using the annual mean MLD.

3 Results

3.1 Sea Ice Response

We first examine the mean state of the Antarctic sea ice area and the response to additional Antarctic meltwater in each of the models that have contributed Tier 1 experiment output to SOFIA. The mean-state annual-mean Antarctic sea ice area in the *piControl* run for each model over the same time period as the *antwater* experiment is shown in Figure 1a. The mean-state Antarctic sea ice area ranges from ~ 6 million km^2 in EC-Earth3 to ~ 14 million km^2 in CanESM5, more than a factor of two difference. As a point of reference, the annual-mean observed Antarctic sea ice area from the NSIDC Sea Ice Index over the satellite era (1979–2024) is 8.7 million km^2. There is a wide range in the response of the Antarctic sea ice area to additional meltwater, with almost no change in AWI-ESM-1-REcoM and a change of ~ 4 million km^2 in CanESM5 and GFDL-ESM4 by year 100 (Figure 1b). This range in sea ice area response can be explained in part by the differing mean state of the Antarctic sea ice area across the models. When the response of the sea ice area is plotted as a percentage change relative to the Antarctic sea ice area in the control run of each model (Figure 1c), there is a 20–40% increase in sea ice area relative to the control by year 100 in most models. The exceptions to this are AWI-ESM-1-REcoM, with very little sea ice area change, and GFDL-ESM4 which has a period of unusually large sea ice area change. This large sea ice area response in the GFDL-ESM4 model, particularly from years 50–70, is influenced by a period of strong open-ocean deep convection present during those years in the *piControl* simulation due to a Ross Sea polynya that occurs in the *piControl* run (see Fig. 5 in Beadling et al., 2022). This

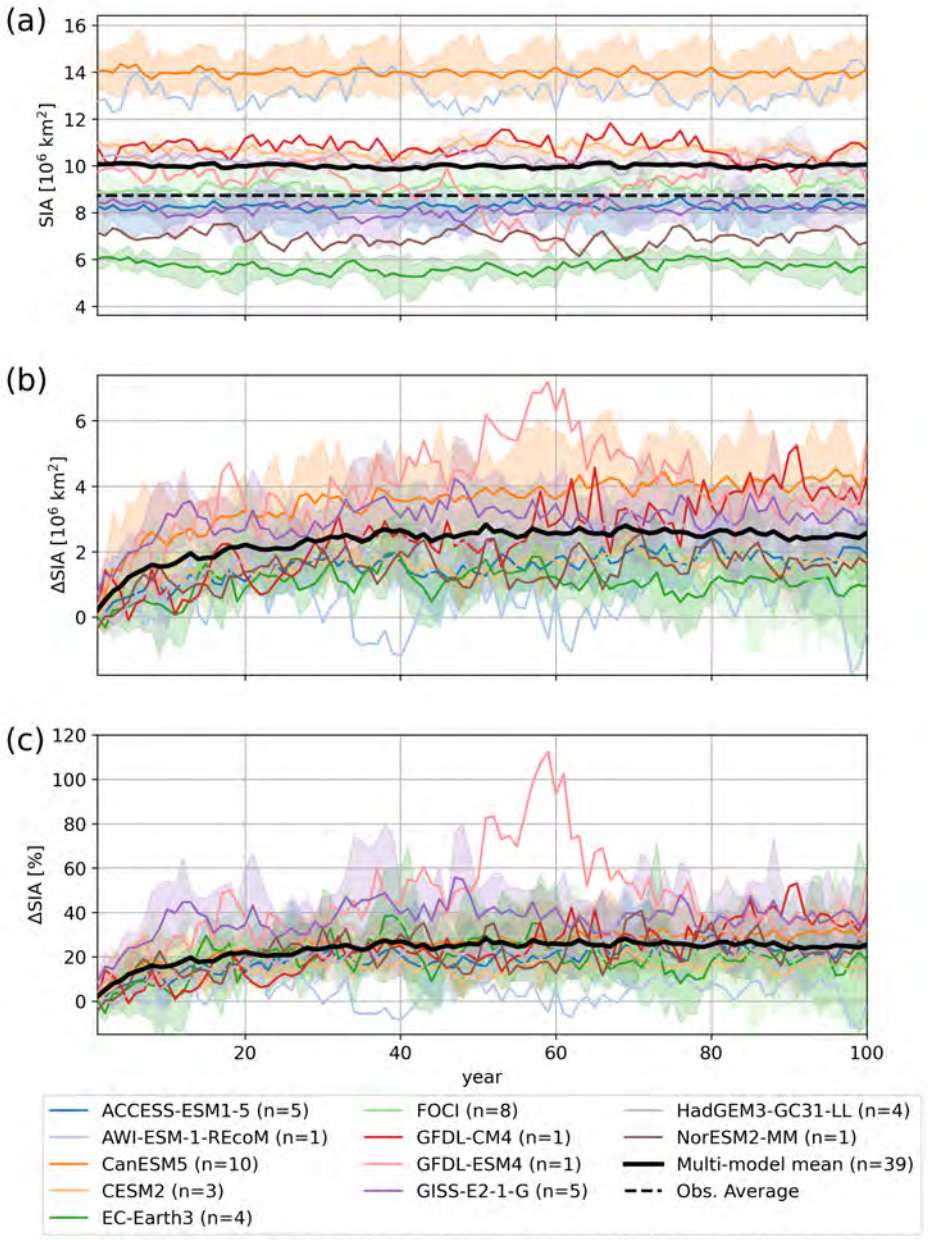

Figure 1. Antarctic annual sea ice area: (a) mean-state in the control run; response as (b) absolute area increase; and (c) percentage change relative to the control run for each of the SOFIA models. Shading denotes the range across ensemble members for the models with more than one ensemble member. Solid colored lines denote each model's ensemble mean. The thick black line denotes the multi-model mean computed by averaging over all ensemble members. The dashed black line shows the average Antarctic sea ice area over the satellite era (1979–2024) as a point of reference (Fetterer et al., 2025).

polynya is not present in the *antwater* simulation, and differencing the time series year-by-year accounts for the ∼2.5 million km^2 variation (dip in sea ice area in *piControl* (Figure 1a) becomes a peak in the response (Figure 1b-c)). The role of open-ocean deep convection in the sea ice response is discussed in more detail below. The ensemble-mean changes in total Antarctic sea ice area and sea ice volume averaged over the last 30 years of the 100-year simulations are summarized in Table 2.

The timescale of the response of the sea ice area to additional Antarctic meltwater also differs between models. In most models, there is an initial rapid increase in sea ice area which later slows and approaches a new equilibrium. However, not all models follow this pattern, with very little change in sea ice area in AWI-ESM-1-REcoM, and an almost monotonic increase over the entire 100 year period in GFDL-CM4. To quantify these differences, we fit an exponential function of the form

$$\Delta\text{SIA} = A\left(1 - e^{\frac{-t}{\tau}}\right) \tag{2}$$

to the ensemble-mean, annual mean sea ice area response, where A is the amplitude in million km^2, t is time in years, and τ is a time constant in units of years. τ represents the time to reach 63% of the final equilibrium value, and the value of τ for each model is given in Table 2. The time constant τ ranges from 0.89 years in AWI-ESM-1-REcoM (in which there is essentially no change in the sea ice area) to 69.2 years in GFDL-CM4, reflecting the almost monotonic increase in sea ice area in that model. Most of the models have τ values between 5 and 20 years, and the multi-model mean value of τ is 10.2 years (see Appendix A for details).

We next examine the mean-state seasonality of the sea ice area and its response to meltwater (Figure 2). In all models, Antarctic sea ice reaches its minimum area in February–March, and its maximum area in September. However, the annual minimum sea ice area varies from almost zero in EC-Earth3, GFDL-CM4, GFDL-ESM4 and GISS-E2-1-G, to more than 5 million km^2 in CanESM5. Although it has the largest annual mean Antarctic sea ice area (Figure 1a), we see that the annual maximum area in CanESM5 (∼20 million km^2) is similar to several other models (AWI-ESM-1-REcoM, GFDL-CM4, GFDL-ESM4). In most models, the increase in sea ice area is largest around the time of the annual sea ice area maximum in September, with a much smaller increase around the time of the annual minimum in February. However, in CanESM5 and FOCI the increase in the sea ice area is approximately the same year-round.

Surface cooling induced by the addition of meltwater from the Antarctic ice sheet can increase not only the areal coverage of sea ice but also its volume. Changes in sea ice volume are important for ocean–atmosphere fluxes of heat, moisture, and carbon as well as biology in this region; thus, we next examine the response of sea ice volume to Antarctic meltwater. Antarctic sea ice volume has a similar large inter-model spread in the *piControl* mean state as the sea ice area (Fig. 3a). There is also a large inter-model spread in the response to Antarctic meltwater. The total volume of sea ice increases by $\sim 8 \times 10^3$ km^3 in CanESM5, while it is relatively unchanged in AWI-ESM-1-REcoM (Fig. 3b). When plotted as a percentage change, we see that the multi-model mean change in sea ice volume is a 42% increase. The two GFDL models have a much higher and more variable percentage change in sea ice volume. In particular, three of the models with low total sea ice volume in their *piControl* runs (GFDL-CM4, GFDL-ESM4 and GISS-E2-1-G) show the largest percentage change in both the area and volume of the sea ice.

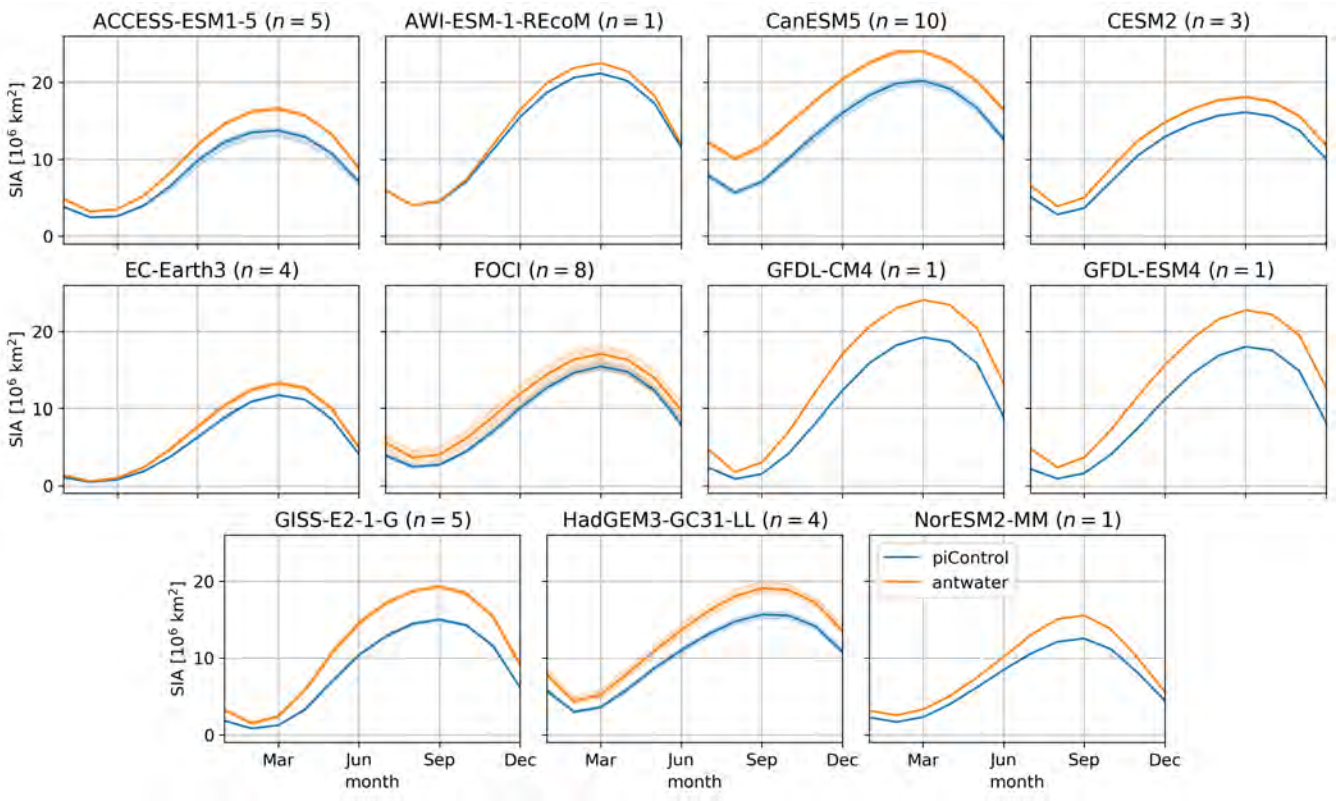

Figure 2. Ensemble-mean seasonal cycle of Antarctic sea ice area for each model. Results are computed as the total Antarctic sea ice area for each month averaged over the final 30 years of the 100 year simulations. The *piControl* is shown in blue and *antwater* is shown in orange. Shading denotes the range across ensemble members for the models with more than one ensemble member.

Due to the different sizes of the ensembles between the models used in this study, it is worth considering the role of the ensemble size in assessing the response. In Appendix B we reproduce Figures 1 and 5 using the first ensemble member only for each model (Figures B1 and B2). Using a single ensemble member for each model does not substantially change any of the qualitative results described above. Thus, we continue to show ensemble mean responses in the main text, as this reduces the role of internal variability in the response. We further conclude that the spread in the response to the freshwater is dominated by model uncertainty since, firstly, the ensemble spread for a given model is typically smaller than the spread across models and, secondly, removing ensemble members does not significantly alter the multi-model mean.

There is a large spread in both the magnitude and spatial pattern of the response of sea ice concentration to the addition of meltwater (Figure 4). The sea ice concentration increases by $\sim 40\%$ in some regions in the CanESM5, GFDL-CM4 and GFDL-ESM4 models. In most models, there is a large change in sea ice concentration near the sea ice edge in the Ross Sea and Amundsen/Bellingshausen Sea regions (between 150–300°E in the lower panel of Figure 4), with little consistency in the pattern response in other regions. The decrease in sea ice concentration in the Lazarev/Rilser-Larsen Sea region in the FOCI

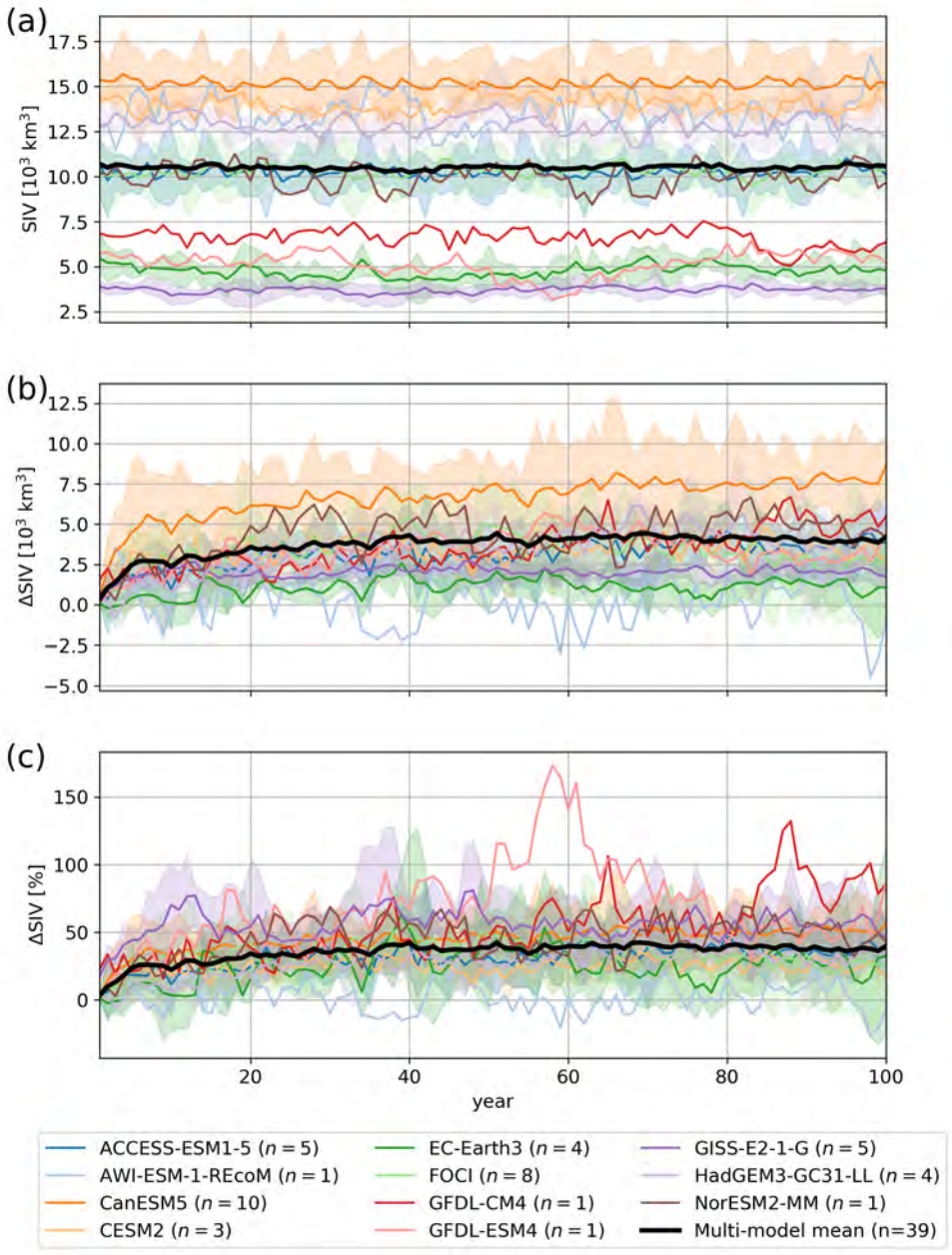

Figure 3. Antarctic annual sea ice volume: (a) mean-state in the control run; response as (b) absolute area increase; and (c) percentage change relative to the control run for each of the SOFIA models. Shading denotes the range across ensemble members for the models with more than one ensemble member. Solid colored lines denote each model's ensemble mean. The thick black line denotes the multi-model mean computed by averaging over all ensemble members.

Model	ΔSIA [10^6 km^2]	ΔSIA [%]	ΔSIV [10^3 km^3]	ΔSIV [%]	τ [yrs]
ACCESS-ESM1-5	1.91 (1.72–2.22)	23.3 (20.4–29.1)	3.80 (3.37–4.38)	37.5 (32.0–43.0)	15.3
AWI-ESM-1-REcoM	0.71	5.6	0.38	3.5	0.89
CanESM5	4.14 (3.76–4.54)	30.0 (26.5–33.7)	7.59 (6.94–8.28)	50.6 (44.8–55.7)	12.2
CESM2	1.73 (1.62–1.90)	16.4 (15.3–17.9)	3.58 (3.35–3.85)	25.8 (24.0–27.8)	7.44
EC-Earth3	0.98 (0.81–1.15)	17.7 (15.1–19.8)	1.12 (0.81–1.47)	24.7 (18.1–30.0)	10.4
FOCI	1.63 (0.08–2.90)	18.5 (1.03–32.9)	2.97 (0.60–4.82)	29.9 (6.27–46.7)	6.13
GFDL-CM4	3.70	35.4	4.72	76.3	69.2
GFDL-ESM4	3.81	39.2	3.25	59.0	13.5
GISS-E2-1-G	3.10 (2.91–3.34)	38.3 (36.0–41.4)	2.07 (1.98–2.20)	55.3 (53.5–58.9)	4.92
HadGEM3-GC31-LL	2.58 (1.65–3.16)	25.7 (16.1–30.7)	4.38 (2.43–5.86)	34.2 (19.0–45.3)	20.80
NorESM2-MM	1.73	25.0	5.08	51.4	11.30
Multi-model mean	2.65 (0.08–4.54)	25.9 (1.03–41.4)	4.07 (0.38–8.28)	40.0 (3.46–76.3)	10.24

Table 2. Ensemble-mean absolute and percentage changes in Antarctic sea ice area (SIA) and sea ice volume (SIV), and time constant τ for an exponential fit to the response. The absolute and percentage changes for each model are averaged over the last 30 years of 100 year simulations. Numbers in parentheses denote the minimum and maximum change across ensemble members for the last 30 years for models with more than one ensemble member.

and EC-Earth3 models is due to the development of a region of open-ocean deep convection, leading to the formation of a large polynya. There are also some regions of reduced sea ice concentration that are associated with open-ocean deep convection in the NorESM2-MM model (Weddell and Ross seas) and to an even smaller degree in ACCESS-ESM1-5 and AWI-ESM-1-REcoM. Nevertheless, even in sectors affected by this decrease in sea ice concentration within the ice pack, a northward expansion of the sea ice edge is found.

The spatial response of the Antarctic sea ice volume also varies widely between models (Figure 5). Several models have a large increase in sea ice volume along the coast in the Indian and Atlantic sectors, extending northward and eastward from the tip of the Antarctic peninsula (300–350°E in the lower panel of Figure 5). Other than in the Weddell Sea/Antarctic Peninsula region, the change in sea ice volume appears to be more homogeneous across models than that in sea ice area.

3.2 Ocean Response

To investigate the reasons for the spread between models in the sea ice response, we first examine the response of sea surface temperature (SST) to the addition of freshwater (Figure 6). There is cooling of the Southern Ocean sea surface in all models, predominantly just beyond the sea ice edge, with a large spread in the magnitude of the cooling. As expected, the models that cool most strongly (CanESM5, GFDL-CM4, GFDL-ESM4 and GISS-E2-1-G) have the largest sea ice concentration and area response (Figure 1b and 4). There is slight warming of the sea surface in the sea ice-covered region in AWI-ESM-1-REcoM,

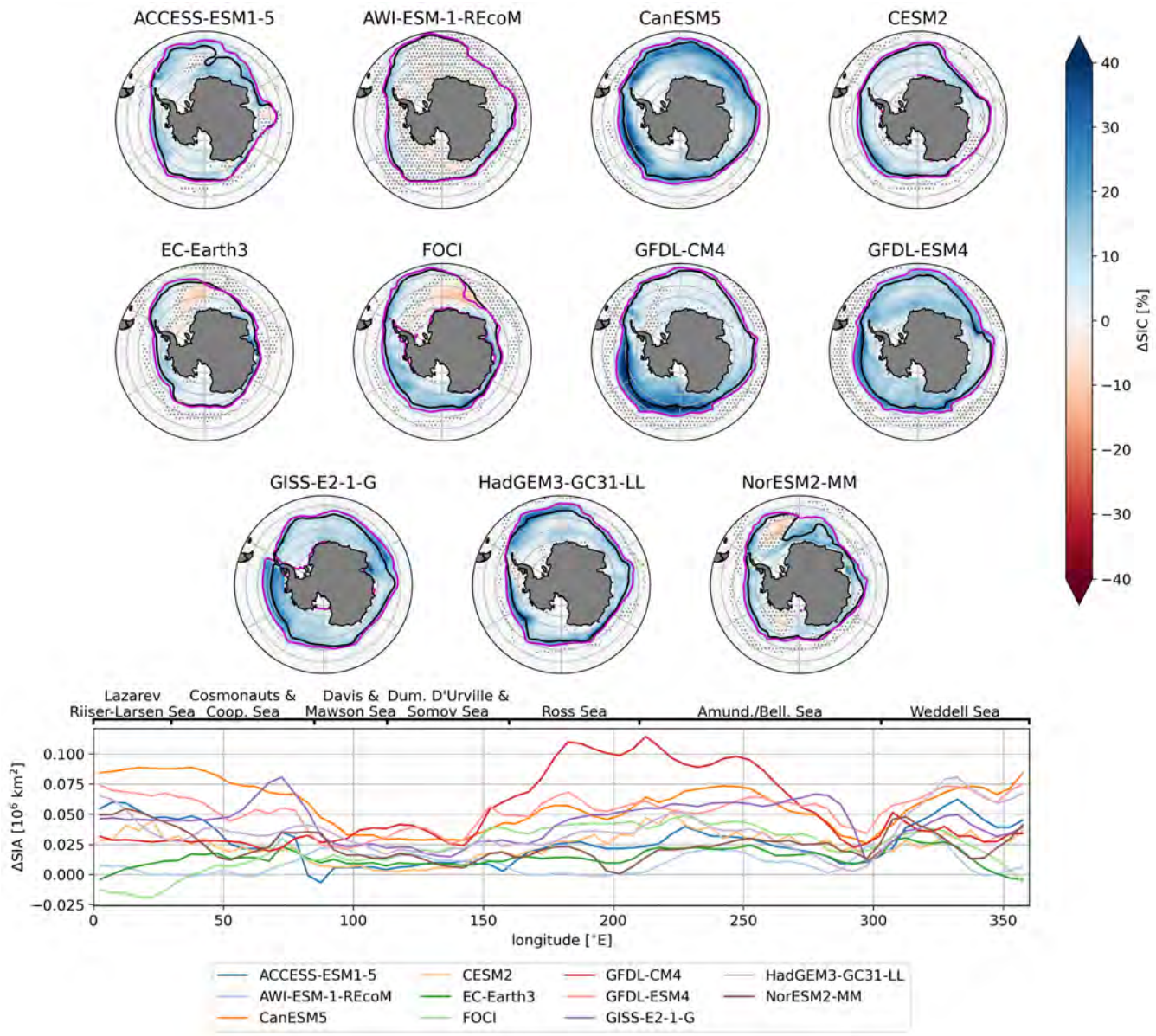

Figure 4. Ensemble-mean sea ice concentration response for each of the models (top three rows). The black and magenta lines denote the annual-mean 15% concentration contour for the *piControl* and *antwater* experiments, respectively. Stippling denotes where the anomaly is not statistically significant at the 95% confidence level. (Bottom row) sea ice area response as a function of longitude. Response is the ensemble-mean difference between the *antwater* experiment and the *piControl* binned into 5 degree longitude increments. Results are averaged over the last 30 years of 100 year simulations.

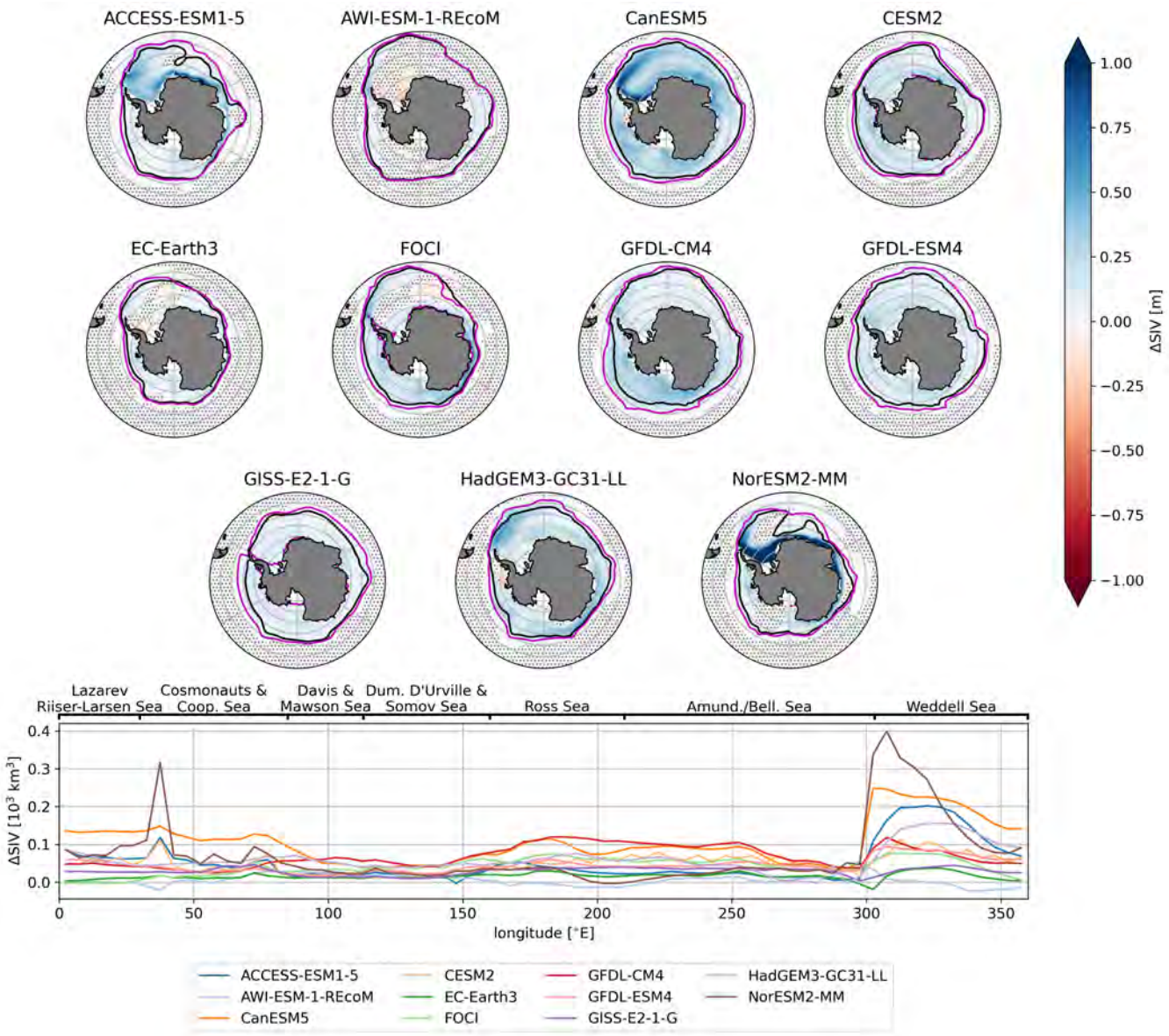

Figure 5. Ensemble-mean sea ice volume response for each of the models (top three rows). The black and magenta lines denote the annual-mean 15% concentration contour for the *piControl* and *antwater* experiments, respectively. Stippling denotes where the anomaly is not statistically significant at the 95% confidence level. (Bottom row) sea ice volume response as a function of longitude. Response is the ensemble-mean difference between the *antwater* experiment and the *piControl* binned into 5 degree longitude increments. Results are averaged over the last 30 years of 100 year simulations.

which is consistent with the weak sea ice response in that model. There are also regions of warming in the FOCI and EC-Earth3 models, consistent with the deep convection that arises in the *antwater* simulation in those models.

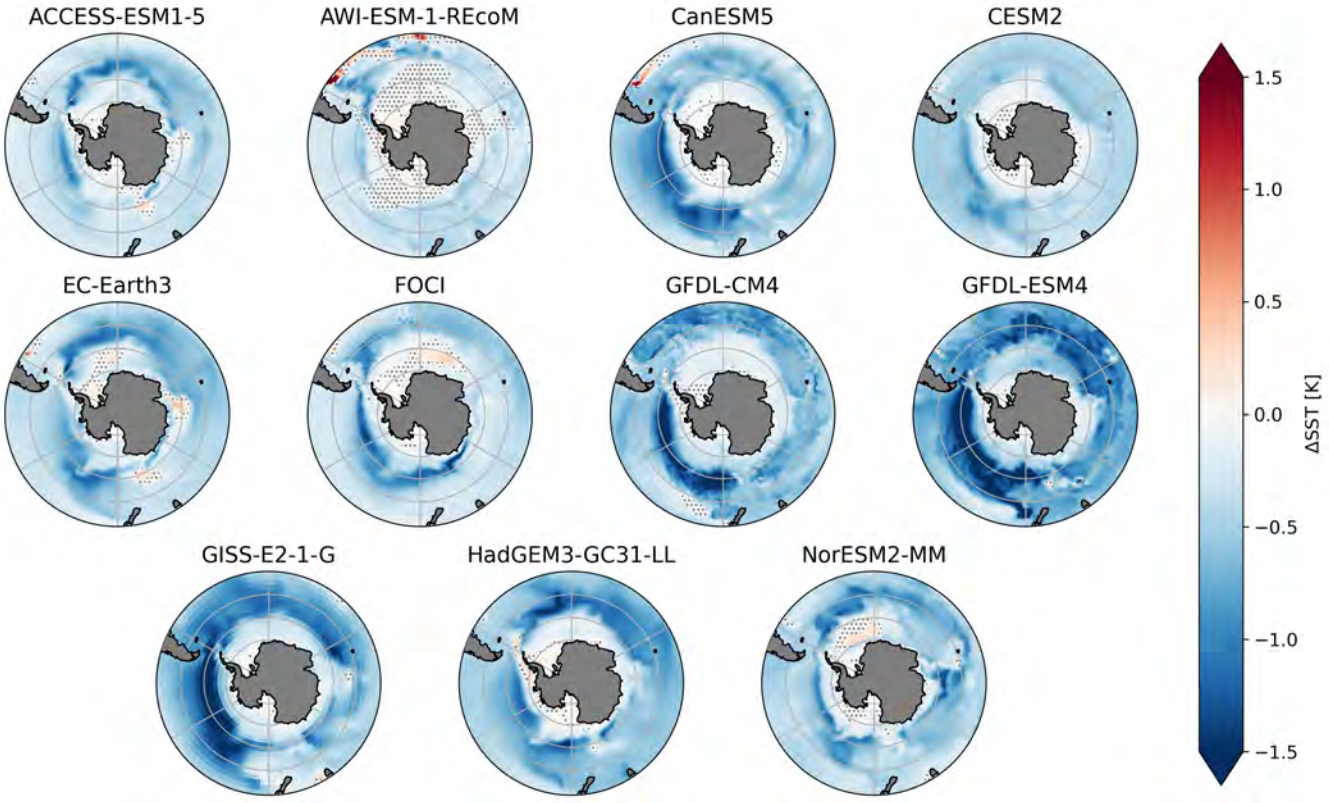

Figure 6. Ensemble-mean annual-mean sea surface temperature response for each of the models. Results are presented as the average over the last 30 years of the 100 year simulations. Stippling denotes where the response is not statistically significant at the 95% confidence level.

Next, we examine the sea surface salinity response (Figure 7). There is a wide range in both the spatial pattern and magnitude of the salinity response across models. There is general surface freshening overall, with some models showing regions of increased salinity (CanESM5, EC-Earth3, FOCI, and GFDL-ESM4 in particular) due to increased brine rejection from sea ice formation. In several models (ACCESS-ESM1-5, EC-Earth3, FOCI, HadGEM3-GC31-LL, and NorESM2-MM), the flow of the meltwater into the South Atlantic from the tip of the Antarctic Peninsula can be seen, consistent with the increased sea ice volume in that region.

Antarctic sea ice is strongly influenced by regions of open-ocean deep convection (e.g., de Lavergne et al., 2014), since the convection mixes relatively warmer, deeper water up to the ocean surface where it can reduce sea ice cover. CMIP6 models exhibit a large spread in the area and location of open-ocean deep convection in their mean-state (Heuzé, 2021). The study of Chen et al. (2023) examined the deep convection response of the Southern Ocean to Antarctic meltwater in a subset of the SOFIA models used in this study. They found that in general the addition of meltwater reduces the amount of deep convection in the SOFIA models due to the meltwater increasing the stratification of the water column. This increase in stratification should in turn result in an increase in sea ice, and so we hypothesize that models with a large reduction in open-ocean deep

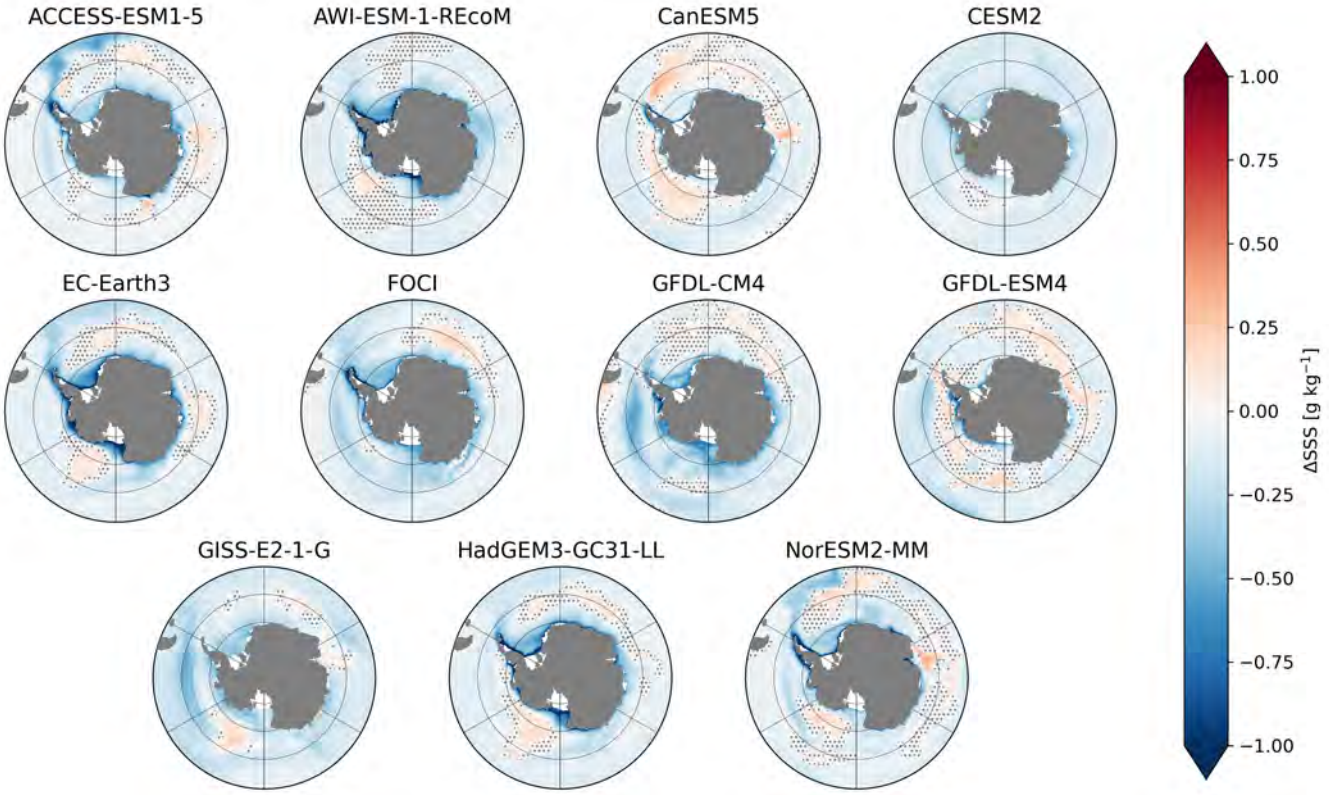

Figure 7. Ensemble-mean annual-mean sea surface salinity response for each of the models. Results are presented as the average over the last 30 years of the 100 year simulations. Stippling denotes where the response is not statistically significant at the 95% confidence level.

convection may have a greater increase in sea ice area or volume. Here, we extend the analysis of Chen et al. (2023) to include four additional models that have contributed simulations to the SOFIA project since that publication. We see a wide range in both the mean state and the response of the total deep mixed volume in the models (Figure 8). About half of the models have little or no open-ocean deep convection in either the *piControl* or *antwater* experiment. Two models, AWI-ESM-1-REcoM and CESM2 have no deep convection at all, and have correspondingly weak sea ice responses. In CanESM5, GFDL-CM4, GFDL-ESM4 and GISS-E2-1-G the addition of Antarctic meltwater shuts off deep convection almost completely. In EC-Earth3, FOCI and HadGEM3-GC31-LL deep mixed volume is reduced for most of the 100 year runs, but regions of deep convection appear in the *antwater* simulation near the end of the century (in all 4 ensemble members for EC-Earth3, in 3 out of 8 ensemble members for FOCI and in 1 out of 4 ensemble members for HadGEM3-GC31-LL). Finally, in ACCESS-ESM1-5 and NorESM2-MM there are large regions of consistent deep convection throughout both the *piControl* and *antwater* experiments throughout the simulation period; however, the DMV is modestly reduced with the addition of meltwater and is accompanied by a corresponding modest increase in the area and volume of sea ice.

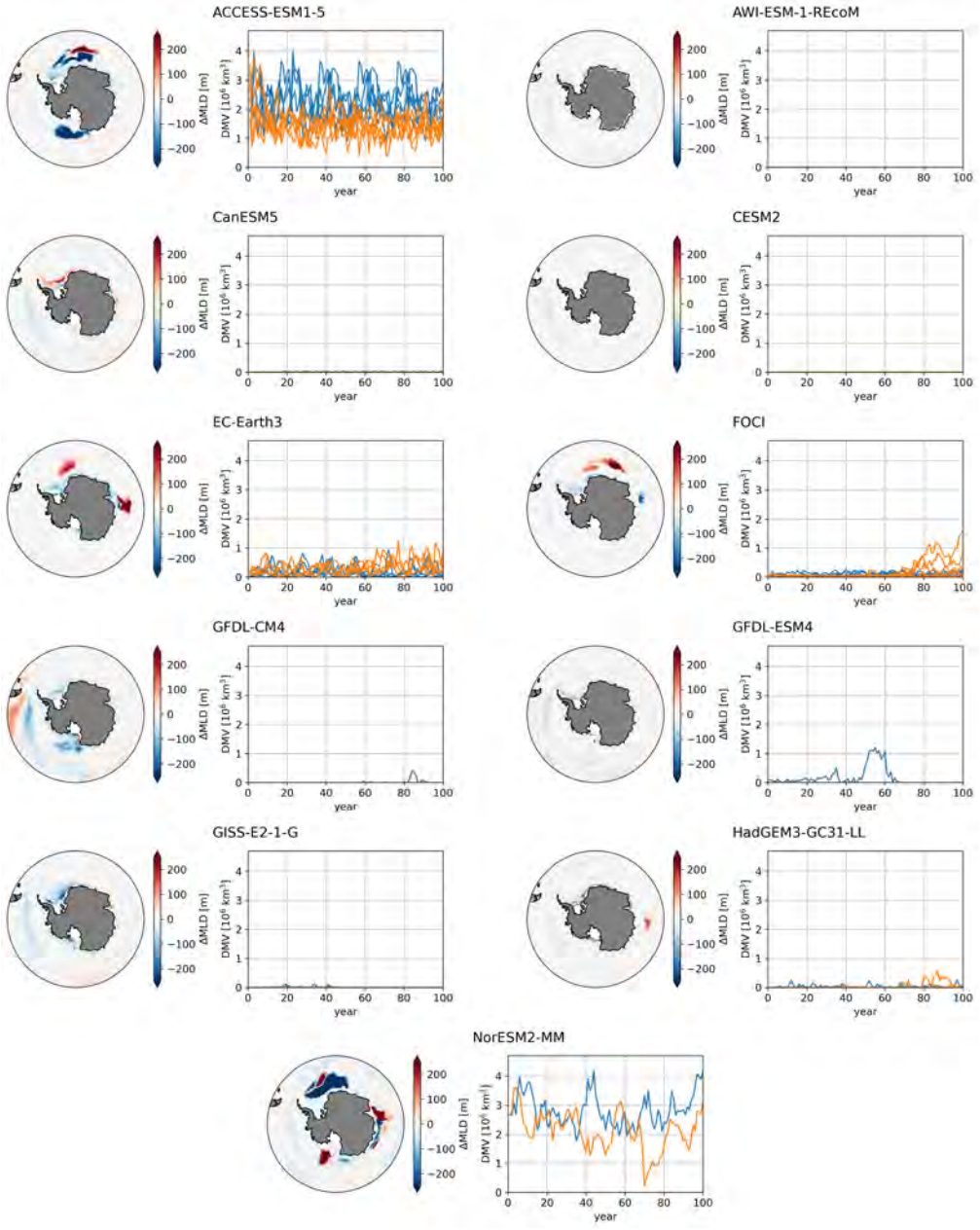

Figure 8. Annual-mean mixed-layer depth response and deep mixed volume (DMV) for the *piControl* (blue) and *antwater* (orange) experiments for each of the models. DMV is computed as the product of mixed-layer depth and grid cell area for all grid cells south of 55°S with mixed-layer depth greater than 2000 m. Mixed-layer depth response is the difference between *antwater* and *piControl* averaged over the final 30 years of 100-year simulations.

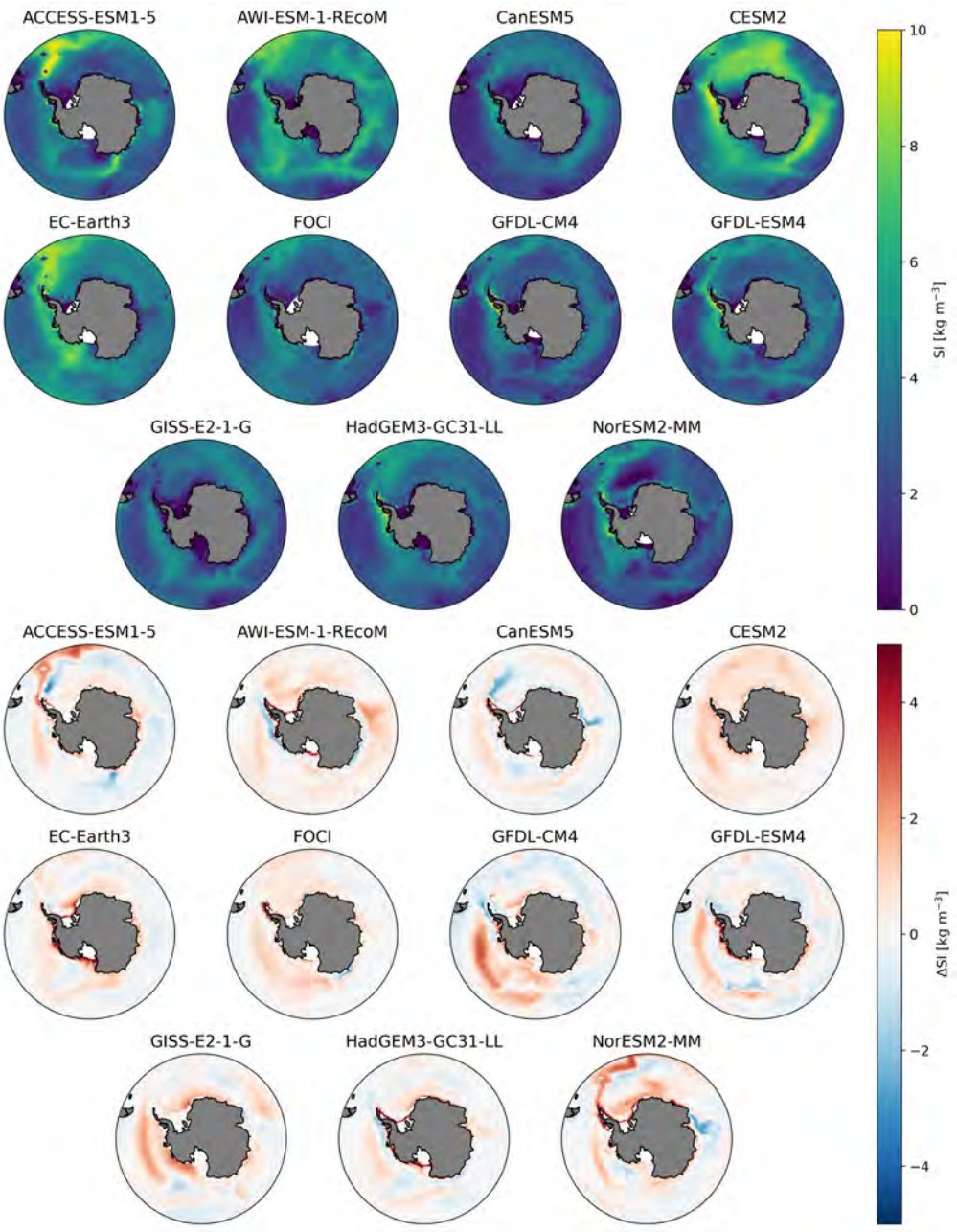

Figure 9. Ensemble-mean stratification index for the *piControl* (top three rows) and the anomaly between the *antwater* experiment and the *piControl* (bottom three rows) for each of the models. A positive anomaly denotes that the water column is becoming more stratified. Results are averaged over the last 30 years of the 100 year simulations.

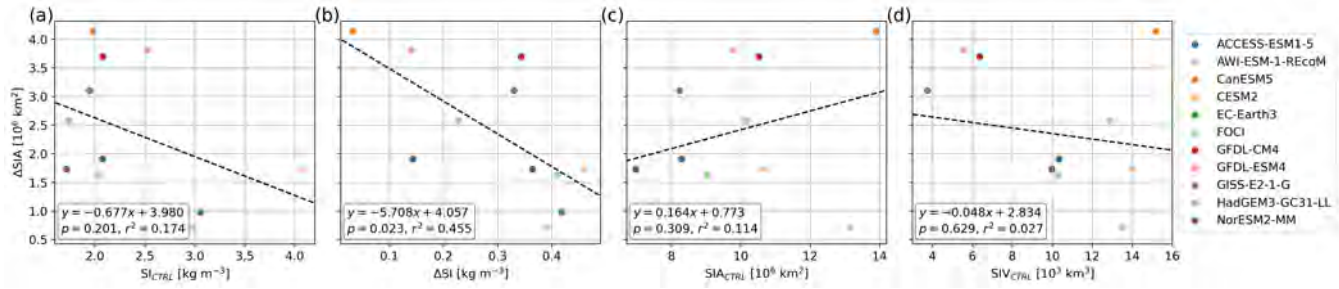

Figure 10. Relationship between the ensemble-mean Antarctic sea ice response and the ensemble-mean *piControl* stratification index (a), the ensemble-mean stratification index response (b), the ensemble-mean *piControl* Antarctic sea ice area (c), and the ensemble-mean *piControl* sea ice volume (d). The result of a linear least-squares fit to the data and the associated p-value are given in the box in the lower left corner of each panel.

The addition of Antarctic meltwater affects sea ice by changing the stratification of the water column (e.g., Fogwill et al., 2015; Pauling et al., 2016; Bronselaer et al., 2018). The increase in stratification due to the addition of relatively fresh, less dense water near the surface results in reduced vertical transport of heat from the deeper ocean to the surface, and inhibits open-ocean deep convection (Chen et al., 2023), both of which result in increased sea ice. In addition, dense brine is rejected during sea ice formation, which counteracts the freshening from meltwater and reduces stratification. We next examine the relationship between stratification and the sea ice response across models. Figure 9 shows the modified stratification index (Equation 1) for both the *piControl* mean state and the anomaly with the addition of meltwater. We see that there is a wide range in both the magnitude and the spatial pattern of ocean stratification in the mean state, and an overall increase in stratification around the continent with the addition of meltwater. In Figure 10 we compute the relationships between the Antarctic sea ice area response (ΔSIA) and the *piControl* stratification index ($\mathrm{SI_{CTRL}}$), the change in stratification index (ΔSI), the *piControl* Antarctic sea ice area ($\mathrm{SIA_{CTRL}}$), and the *piControl* Antarctic sea ice volume ($\mathrm{SIV_{CTRL}}$). The relationship between ΔSIA and ΔSI is statistically significant ($p < 0.05$), suggesting that the magnitude of the increase in stratification and the sea ice response are tightly coupled. We find no statistically significant relationships at the 95% confidence level between the Antarctic sea ice area response and the mean-state stratification index, the mean-state sea ice area, or the mean-state sea ice volume. In addition, these relationships help explain some of the intermodel spread in the sea ice response. The two most strongly stratified models, AWI-ESM-1-REcoM and CESM2 (Figure 10a), have the weakest sea ice response and no deep mixing. We also examined the mean state and response of the stratification seasonally, but found no clear seasonal dependence in the response (not shown).

4 Discussion

In this study, we present results from the first coordinated multi-model ensemble to examine the response of sea ice to meltwater resulting from Antarctic ice sheet mass loss. We find that multiple factors contribute to the wide inter-model spread in both the temporal and spatial response. The mean-state sea ice area in the *piControl* simulations for each model explains some of the

spread: those models with larger mean-state Antarctic sea ice area also generally (though not always) have a larger change in area in response to meltwater. Furthermore, the models with the thinnest mean state sea ice in their *piControl* runs have the largest percentage changes in sea ice area and volume. This indicates that models with thin sea ice are more sensitive to surface cooling driven by the addition of the meltwater and are able to grow more ice because of the reduced insulating effect of the existing sea ice. We found no obvious overall relationship between the method of computing the freezing point of seawater and the sea ice response across models (not shown). However, we note that AWI-ESM-1-REcoM, the only model with a fixed freezing point temperature calculation, had a particularly weak sea ice response. This may be in part due to the inability of the freezing point of seawater to response to changes in salinity in this model.

The spatial response of sea ice concentration (Figure 4) is consistent with ocean model simulations of meltwater release (see supporting information of Ashley et al., 2021) showing that meltwater released as far away from the Peninsula as the Ross Ice Shelf front follows the Antarctic coastal and slope currents anticlockwise around the continent, before separating at the tip of the Antarctic Peninsula. Some of the meltwater continues around the Antarctic coast, with the remainder flowing into the Weddell Gyre and out into the Atlantic Ocean, in a pattern similar to the sea ice volume changes shown here. This means that some fraction of much of the meltwater released all around the Antarctic continent will end up being entrained into the Weddell Gyre and flowing into the South Atlantic. Thus, a disproportionate amount of the freshening and stratifying effect of the meltwater will be present in this region.

In most models the sea ice increase is largest in winter and smallest in summer (Figure 2). This may be linked to the mechanisms by which meltwater influences sea ice. Sea ice formation requires that the seawater near the surface is cooled to the freezing point. The volume of water that needs to be cooled is dependent on the mixed-layer depth and hence the stratification, and thus the winter sea ice may be more strongly influenced by additional meltwater. Conversely, in summer the sea ice is melting and freshening the surface regardless of the addition of meltwater, and so may be less influenced by meltwater. For CanESM5 and FOCI the seasonality in sea ice area response is less pronounced, however the difference between *piControl* and *antwater* is slightly smaller during the melt season, and thus consistent with this mechanism.

Ocean stratification and open-ocean deep convection play important roles in influencing the sea ice response. The response in ocean stratification is strongly related to the sea ice response (Figure 10b). There is a wide range of mean-state deep convection behavior of the CMIP6 models in the Southern Ocean (Heuzé, 2021), and the subset of CMIP6 models used here also exhibit this range. We find that models without deep convection have relatively weak sea ice responses. GFDL-ESM4, which experiences a period of deep convection in the *piControl* simulation that is absent in *antwater*, exhibits a pronounced sea ice area anomaly in the middle of the 100-year simulation (Figure 1a,b). Furthermore, in the EC-Earth3, FOCI, and HadGEM3-GC31-LL models, regions of deep convection form near the end of the *antwater* simulation, explaining the reduction in sea ice area observed in those models. This region of deep convection is clearly visible in the Lazarev / Riilser-Larsen Sea region in the sea ice concentration response for the EC-Earth3 and FOCI models (Figure 4). Thus, open-ocean deep convection contributes somewhat to the inter-model spread in the response to Antarctic meltwater.

The response of AWI-ESM-1-REcoM is particularly unusual among the models presented here. Despite having high mean-state sea ice area, high sea ice volume and similar ocean stratification to other models, the sea ice response is very weak.

This is despite having one of the largest sea surface salinity responses across the models (Muilwijk et al., 2025). This model differs from the others in the ensemble due to having a refined ocean grid close to the Antarctic coastline, with a grid spacing of approximately 20 km near the Antarctic coast, which becomes coarser to the north. Investigation of the reasons for the unusually weak apparent coupling between the ocean and sea ice responses in this model are ongoing.

The *antwater* experiment as defined in the SOFIA protocol (Swart et al., 2023) has many simplifications that should be considered when interpreting the results shown here. In this experiment, the meltwater is evenly distributed across all grid cells immediately adjacent to the Antarctic coast, while in the present-day real world and future projections the meltwater input is higher in the Amundsen/Bellingshausen Sea region (Shepherd et al., 2018; Seroussi et al., 2020). Meltwater also enters the ocean surface in *antwater*, whereas in reality much of the input occurs at depth (Rignot et al., 2019). In addition, the latent heat required to melt the ice is not extracted from the ocean; only the freshening effect is included. In reality, meltwater enters the ocean through a combination of basal melting of ice shelves, where the meltwater enters the open ocean at depth, and calving and subsequent melting of icebergs, where the meltwater enters the ocean near the surface but far from the coastline. The effect of the horizontal and vertical spatial distribution of meltwater input has been examined before in individual modelling studies (e.g., Merino et al., 2018; Mackie et al., 2020a, b; Thomas et al., 2023), with important implications for the local oceanic response in particular, such as different vertical profiles of temperature change over the continental shelf regions. The effect and relative importance of the spatial distribution and the inclusion of the latent heat effect will be tested in the Tier 3 experiments defined in the SOFIA protocol in Swart et al. (2023). Nonetheless, the results presented here represent an important first step in understanding the inter-model spread in the response of Antarctic sea ice to meltwater from the ice sheet, and can be built on by this future work.

The results shown demonstrate that care must be taken when interpreting a given model response to Antarctic meltwater. It has been argued that the inclusion of meltwater due to Antarctic ice-sheet mass loss in historical simulations is important for the models' ability to reproduce the observed sea surface temperature and sea ice trends (Schmidt et al., 2023). However, we have shown here that the magnitude of the Antarctic sea ice response to identical meltwater forcing may vary widely by the end of our 100-year simulations. In Tier 2 experiments of the SOFIA protocol, the effect of Antarctic meltwater due to ice sheet mass loss will be tested under historical and future climate forcing, using best estimates of the historical forcing from Slater et al. (2021), and the ice sheet model output from the Ice Sheet Model Intercomparison Project phase 6 (ISMIP6, Seroussi et al., 2020).

5 Conclusions

The work presented here represents the first coordinated multi-model ensemble analysis of the response of Antarctic sea ice to meltwater entering the Southern Ocean due to mass loss from the Antarctic ice sheet. This meltwater is not included in the coupled climate model simulations that currently form the basis for future climate projections, so understanding the magnitude and uncertainty of its potential impact is important. In response to the addition of 0.1 Sv of meltwater distributed evenly around the Antarctic coast at the ocean surface, the total Antarctic sea ice area increases in the 10 models examined here, but ranges

from an annual-mean increase of 0.71–4.14 million km^2 by the end of 100 years. Similarly, annual-mean sea ice volume increases by between 0.38–7.59$\times 10^3$ km^3 across models. There is no single reason for this large intermodel spread, but a combination of the mean-state Antarctic sea ice area, the mean-state vertical stratification in the ocean, and the mean-state and response of open-ocean deep convection explain much of the variability in response. This work highlights the importance of targeted model intercomparison projects for understanding the climate response to a particular forcing and motivates the running and analysis of additional model experiments defined in the SOFIA protocol that will isolate the role of more detailed aspects of Antarctic meltwater input to the Southern Ocean.

Code and data availability. CMIP6 model output is available at https://esgf-node.llnl.gov/projects/cmip6. SOFIA model output is available at https://crd-data-donnees-rdc.ec.gc.ca/CCCMA/SOFIA. The code necessary to reproduce the results of this study is available at Pauling (2026).

Appendix A: Timescale of the sea ice response

Figure A1 shows the exponential fit to the ensemble-mean sea ice area response for each model, following Equation 2. For most models, the response of the sea ice area is well described by the exponential model, the exceptions being AWI-ESM-1-REcoM and GFDL-ESM4. AWI-ESM-1-REcoM has almost no change in the sea ice area with the addition of meltwater, so the exponential fit to the response is not meaningful. GFDL-ESM4 has large variability, suggesting that the exponential model does not fit the data well, due to the presence of a large open-ocean polynya in years 50–70, as discussed in the main text.

Appendix B: Single ensemble member sea ice response

Different numbers of ensemble members were run for each model that contributed output to the *antwater* SOFIA experiment, with several models running only one ensemble member. This means that comparing the ensemble-mean sea ice responses across models in Figures 1 and 5 is not a direct comparison. Thus, in Figures B1 and B2 we compute the sea ice area and volume responses, respectively, using the first ensemble member from each model (variant label *r1i1p1f1* or *r1i1p2f1* depending on the convention used in each model). We see that the responses are qualitatively similar to those seen in the ensemble mean, with the response of the sea ice area ranging from ~ 0 to ~ 4 million km^2 by the end of the century (Figure B1 b) and the sea ice area in most models increases by 20–40% by the end of the century (Figure B1c). Similarly, the sea ice volume response ranges from between $\sim$0 and $\sim$7.5$\times 10^3$ km^3 (Figure B2b) and sea ice volume increases by 25–90% in most models as a percentage of the *piControl* mean state (Figure B2c).

Author contributions. Conceptualization: AGP, IJS; Data curation: AGP, TM, MM, RLB, NCS, CD, QL, AP, MT; Formal analysis: AGP; Writing – original draft: AGP; Visualization: AGP; Writing – review & editing: All authors.

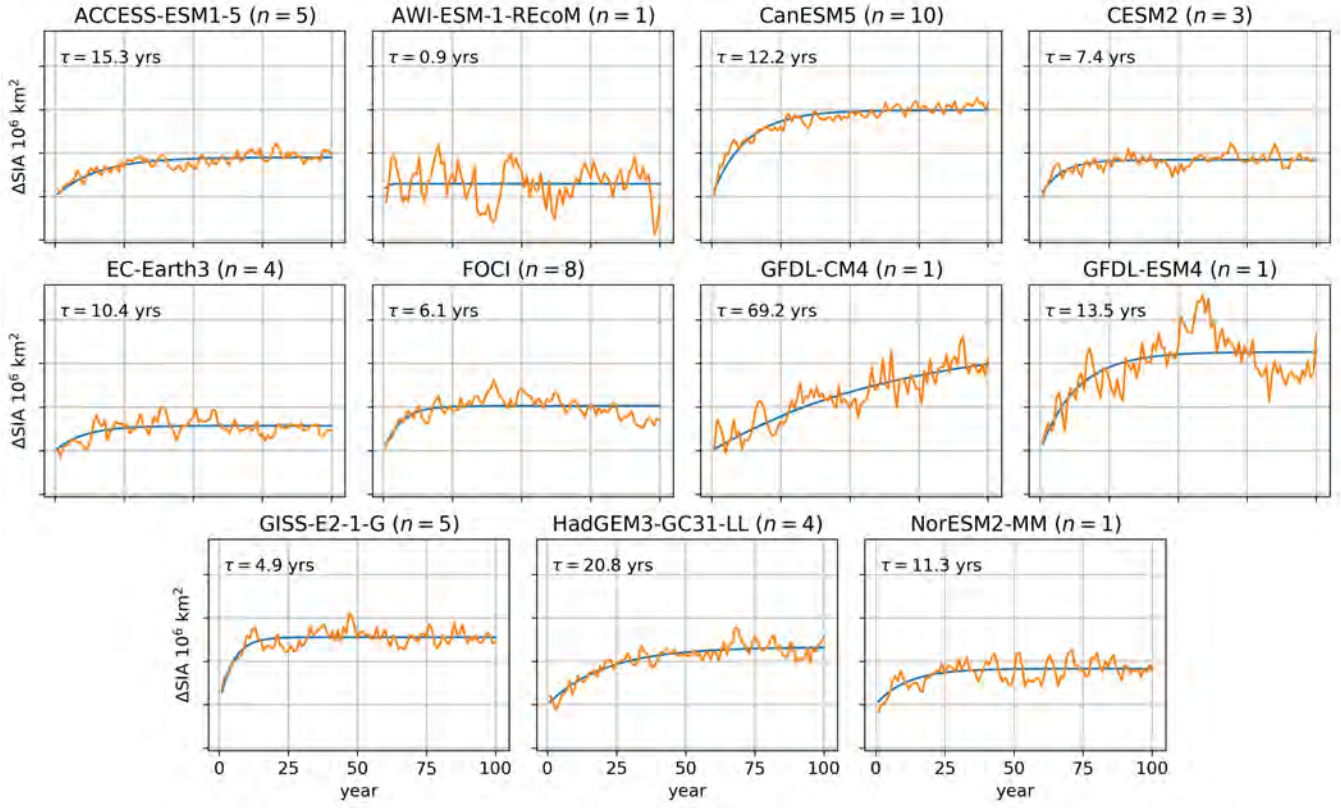

Figure A1. Ensemble-mean Antarctic sea ice area response for each model with an exponential fit to each curve following Equation 2. The time constant τ is given for each model. n denotes the number of ensemble members in each model.

Competing interests. The authors declare no competing interests.

Acknowledgements. AGP, IJS and MT were supported by the New Zealand Deep South National Science Challenge (MBIE contract number C01X1412) and the New Zealand Antarctic Science Platform (University of Otago subcontract 19424 from VUW's ASP Project 4 contract with Antarctica New Zealand through MBIE SSIF Programmes Investment contract number ANTA1801). RLB was supported under NSF Division of Polar Programs Grant NSF2319828. The authors acknowledge preliminary modeling work by Shona Mackie and technical support from Jonny Williams. The authors wish to acknowledge the use of New Zealand eScience Infrastructure (NeSI) high performance computing facilities, consulting support, and/or training services as part of this research. New Zealand's national facilities are provided by NeSI and funded jointly by NeSI's collaborator institutions and through the Ministry of Business, Innovation & Employment's Research Infrastructure programme. URL: https://www.nesi.org.nz. We acknowledge high-performance computing support from Cheyenne (doi:10.5065/D6RX99HX) provided by NCAR's Computational and Information Systems Laboratory, sponsored by the National Science Foundation. The authors thank the Community Earth System Model (CESM) Polar Climate Working Group and the CESM Climate Variability and Change Working Group for computing time on the Cheyenne supercomputer. AP was supported by the Australian Research Council

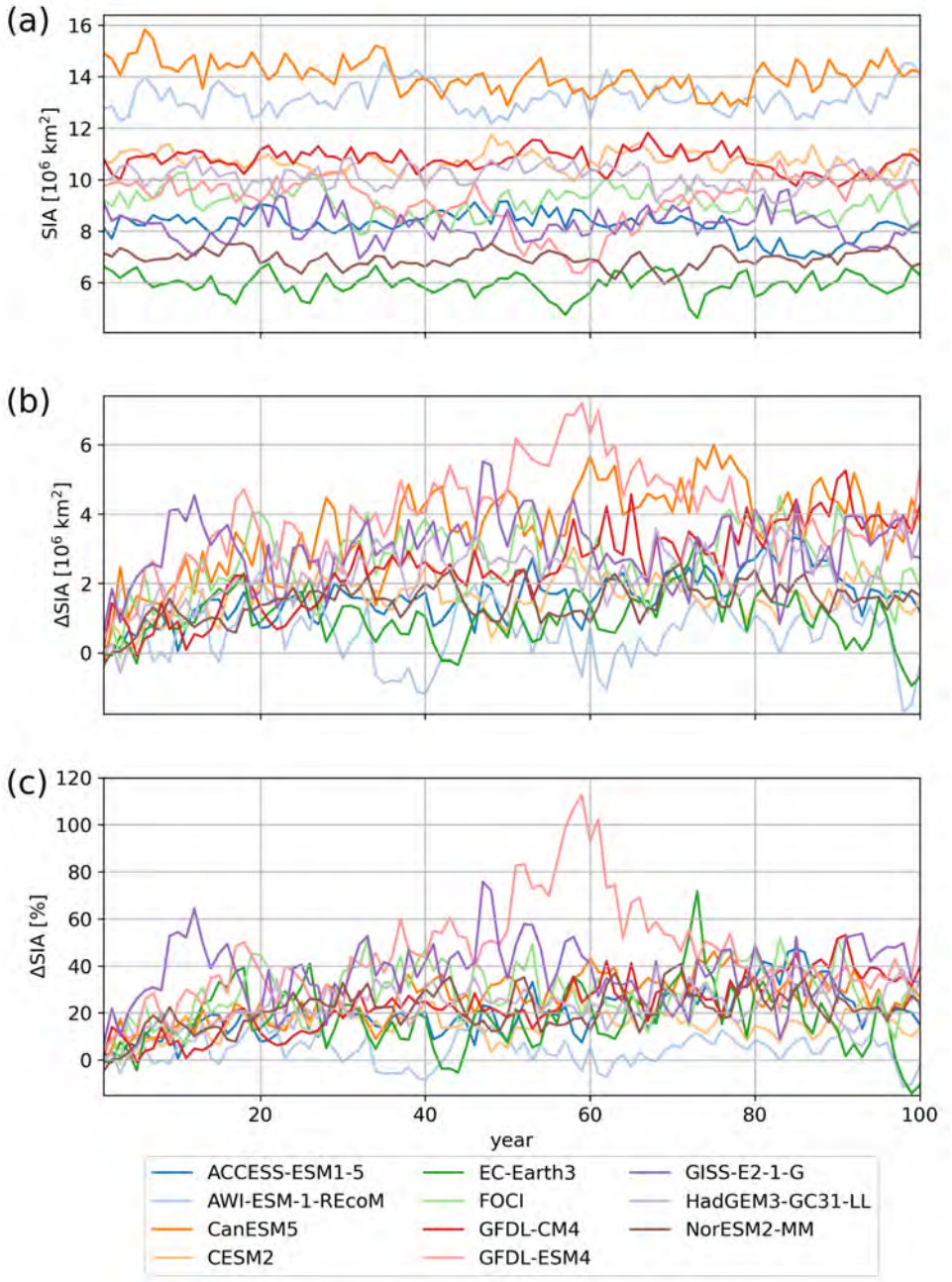

Figure B1. Antarctic sea ice area (a): mean state in the control run, and response as (b): absolute area increase and (c): percentage change relative to the control run for each of the SOFIA models for the first ensemble member in each model. Light-colored lines denote individual ensemble members. Solid colored lines denote each model's ensemble mean.

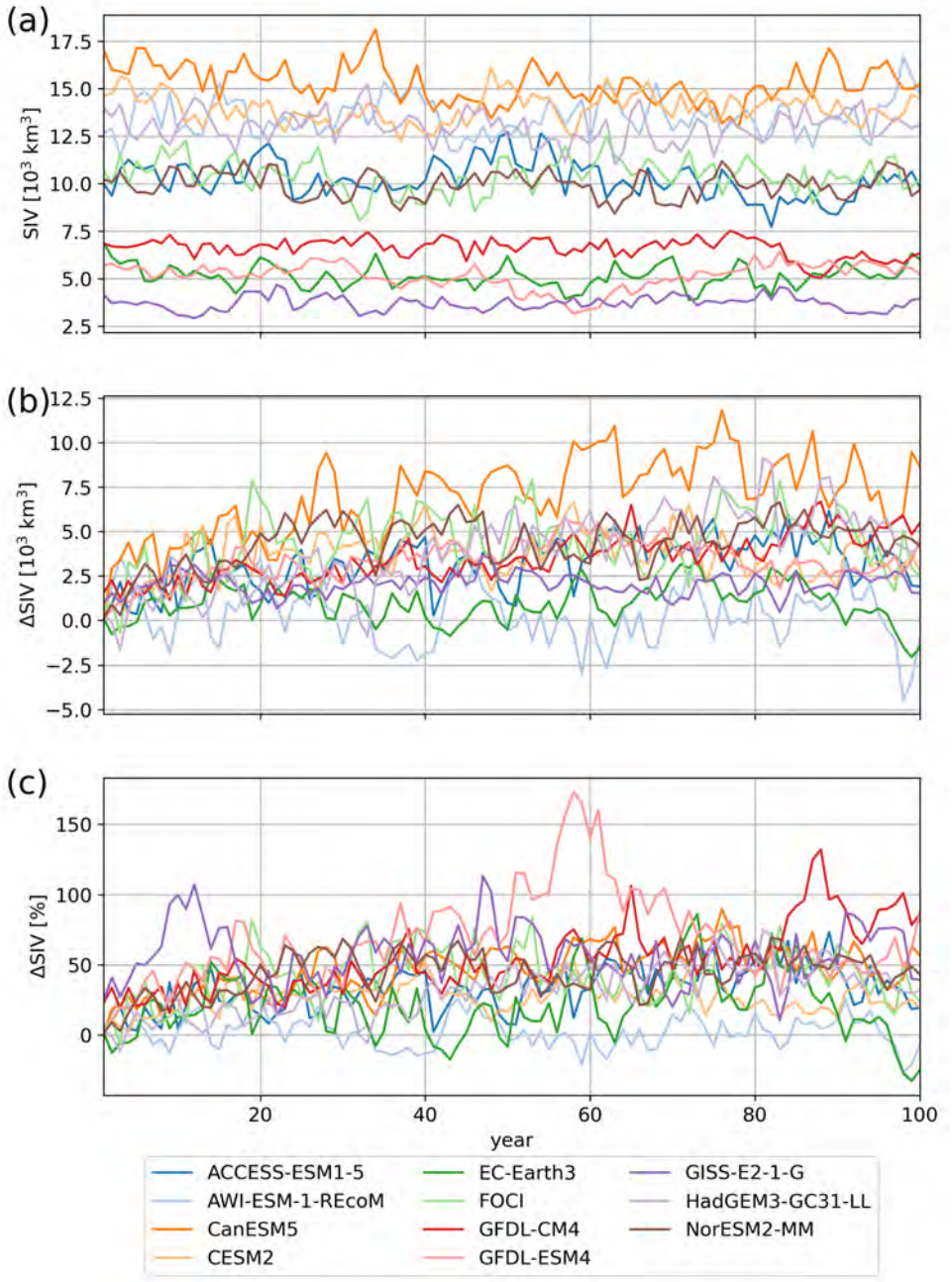

Figure B2. Antarctic sea ice volume (a): mean state in the control run, and response as (b): absolute volume increase and (c): percentage change relative to the control run for each of the SOFIA models for the first ensemble member in each model. Light-colored lines denote individual ensemble members. Solid colored lines denote each model's ensemble mean.

Special Research Initiative for Securing Antarctica's Environmental Future (SR200100005). RLB was supported by NSF Division of Polar Programs grant NSF2319828. MM received funding from the European Union's Horizon 2020 research and innovation programme under grant agreement No 101003826 via project CRiceS. Significant effort has been invested by the SOFIA team to design the experiments, the modelers to run the experiments, and by the project members to house the data in an open common archive. Further details are available at https://sofiamip.github.io and described in Swart et al. (2023). We thank Irene Trombini for providing additional model output for the EC-Earth3 model.

References

Adusumilli, S., Fricker, H. A., Medley, B., Padman, L., and Siegfried, M. R.: Interannual variations in meltwater input to the Southern Ocean from Antarctic ice shelves, Nat. Geosci., 13, 616–620, https://doi.org/10.1038/s41561-020-0616-z, 2020.

Ashley, K. E., McKay, R., Etourneau, J., Jimenez-Espejo, F. J., Condron, A., Albot, A., Crosta, X., Riesselman, C., Seki, O., Massé, G., Golledge, N. R., Gasson, E., Lowry, D. P., Barrand, N. E., Johnson, K., Bertler, N., Escutia, C., Dunbar, R., and Bendle, J. A.: Mid-Holocene Antarctic sea-ice increase driven by marine ice sheet retreat, Climate of the Past, 17, 1–19, https://doi.org/10.5194/cp-17-1-2021, 2021.

Beadling, R. L., Krasting, J. P., Griffies, S. M., Hurlin, W. J., Bronselaer, B., Russell, J. L., MacGilchrist, G. A., Tesdal, J.-E., and Winton, M.: Importance of the Antarctic Slope Current in the Southern Ocean Response to Ice Sheet Melt and Wind Stress Change, J. Geophys. Res.-Oceans, 127, e2021JC017 608, https://doi.org/10.1029/2021JC017608, 2022.

Beadling, R. L., Lin, P., Krasting, J., Ellinger, W., Coomans, A., Milward, J., Turner, K., Xu, X., Martin, T., and Molina, M. J.: From the Surface to the Stratosphere: Large-Scale Atmospheric Response to Antarctic Meltwater, Geophys. Res. Lett., 51, e2024GL110 157, https://doi.org/10.1029/2024GL110157, 2024.

Bintanja, R., van Oldenborgh, G. J., Drijfhout, S. S., Wouters, B., and Katsman, C. A.: Important role for ocean warming and increased ice-shelf melt in Antarctic sea-ice expansion, Nat. Geosci., 6, 376–379, https://doi.org/10.1038/NGEO1767, 2013.

Bintanja, R., Van Oldenborgh, G. J., and Katsman, C. A.: The effect of increased fresh water from Antarctic ice shelves on future trends in Antarctic sea ice, Ann. Glaciol., 56, 120–126, https://doi.org/10.3189/2015AoG69A001, 2015.

Bourgeois, T., Goris, N., Schwinger, J., and Tjiputra, J. F.: Stratification constrains future heat and carbon uptake in the Southern Ocean between 30°S and 55°S, Nat. Commun., 13, 340, https://doi.org/10.1038/s41467-022-27979-5, 2022.

Bronselaer, B., Winton, M., Griffies, S. M., Hurlin, W. J., Rodgers, K. B., Sergienko, O. V., Stouffer, R. J., and Russell, J. L.: Change in future climate due to Antarctic meltwater, Nature, 564, 53–58, https://doi.org/10.1038/s41586-018-0712-z, 2018.

Chen, J.-J., Swart, N. C., Beadling, R., Cheng, X., Hattermann, T., Jüling, A., Li, Q., Marshall, J., Martin, T., Muilwijk, M., Pauling, A. G., Purich, A., Smith, I. J., and Thomas, M.: Reduced Deep Convection and Bottom Water Formation Due To Antarctic Meltwater in a Multi-Model Ensemble, Geophys. Res. Lett., 50, e2023GL106 492, https://doi.org/10.1029/2023GL106492, 2023.

Danabasoglu, G., Lamarque, J.-F., Bacmeister, J., Bailey, D. A., DuVivier, A. K., Edwards, J., Emmons, L. K., Fasullo, J., Garcia, R., Gettelman, A., Hannay, C., Holland, M. M., Large, W. G., Lauritzen, P. H., Lawrence, D. M., Lenaerts, J. T. M., Lindsay, K., Lipscomb, W. H., Mills, M. J., Neale, R., Oleson, K. W., Otto-Bliesner, B., Phillips, A. S., Sacks, W., Tilmes, S., van Kampenhout, L., Vertenstein, M., Bertini, A., Dennis, J., Deser, C., Fischer, C., Fox-Kemper, B., Kay, J. E., Kinnison, D., Kushner, P. J., Larson, V. E., Long, M. C., Mickelson, S., Moore, J. K., Nienhouse, E., Polvani, L., Rasch, P. J., and Strand, W. G.: The Community Earth System Model Version 2 (CESM2), J. Adv. Model. Earth Syst., 12, e2019MS001 916, https://doi.org/10.1029/2019MS001916, 2020.

Davison, B. J., Hogg, A. E., Gourmelen, N., Jakob, L., Wuite, J., Nagler, T., Greene, C. A., Andreasen, J., and Engdahl, M. E.: Annual mass budget of Antarctic ice shelves from 1997 to 2021, Science Advances, 9, eadi0186, https://doi.org/10.1126/sciadv.adi0186, 2023.

de Lavergne, C., Palter, J. B., Galbraith, E. D., Bernardello, R., and Marinov, I.: Cessation of deep convection in the open Southern Ocean under anthropogenic climate change, Nat. Clim. Change, 4, 278–282, https://doi.org/10.1038/nclimate2132, 2014.

Dong, Y., Armour, K. C., Battisti, D. S., and Blanchard-Wrigglesworth, E.: Two-Way Teleconnections between the Southern Ocean and the Tropical Pacific via a Dynamic Feedback, J. Climate, 35, 6267–6282, https://doi.org/10.1175/JCLI-D-22-0080.1, 2022a.

Dong, Y., Pauling, A. G., Sadai, S., and Armour, K. C.: Antarctic Ice-Sheet Meltwater Reduces Transient Warming and Climate Sensitivity Through the Sea-Surface Temperature Pattern Effect, Geophys. Res. Lett., 49, e2022GL101 249, https://doi.org/10.1029/2022GL101249, 2022b.

Dunne, J. P., Horowitz, L. W., Adcroft, A. J., Ginoux, P., Held, I. M., John, J. G., Krasting, J. P., Malyshev, S., Naik, V., Paulot, F., Shevliakova, E., Stock, C. A., Zadeh, N., Balaji, V., Blanton, C., Dunne, K. A., Dupuis, C., Durachta, J., Dussin, R., Gauthier, P. P. G., Griffies, S. M., Guo, H., Hallberg, R. W., Harrison, M., He, J., Hurlin, W., McHugh, C., Menzel, R., Milly, P. C. D., Nikonov, S., Paynter, D. J., Ploshay, J., Radhakrishnan, A., Rand, K., Reichl, B. G., Robinson, T., Schwarzkopf, D. M., Sentman, L. T., Underwood, S., Vahlenkamp, H., Winton, M., Wittenberg, A. T., Wyman, B., Zeng, Y., and Zhao, M.: The GFDL Earth System Model Version 4.1 (GFDL-ESM 4.1): Overall Coupled Model Description and Simulation Characteristics, J. Adv. Model. Earth Syst., 12, e2019MS002 015, https://doi.org/10.1029/2019MS002015, 2020.

Döscher, R., Acosta, M., Alessandri, A., Anthoni, P., Arsouze, T., Bergman, T., Bernardello, R., Boussetta, S., Caron, L.-P., Carver, G., Castrillo, M., Catalano, F., Cvijanovic, I., Davini, P., Dekker, E., Doblas-Reyes, F. J., Docquier, D., Echevarria, P., Fladrich, U., Fuentes-Franco, R., Gröger, M., v. Hardenberg, J., Hieronymus, J., Karami, M. P., Keskinen, J.-P., Koenigk, T., Makkonen, R., Massonnet, F., Ménégoz, M., Miller, P. A., Moreno-Chamarro, E., Nieradzik, L., van Noije, T., Nolan, P., O'Donnell, D., Ollinaho, P., van den Oord, G., Ortega, P., Prims, O. T., Ramos, A., Reerink, T., Rousset, C., Ruprich-Robert, Y., Le Sager, P., Schmith, T., Schrödner, R., Serva, F., Sicardi, V., Sloth Madsen, M., Smith, B., Tian, T., Tourigny, E., Uotila, P., Vancoppenolle, M., Wang, S., Wårlind, D., Willén, U., Wyser, K., Yang, S., Yepes-Arbós, X., and Zhang, Q.: The EC-Earth3 Earth system model for the Coupled Model Intercomparison Project 6, Geosci. Model Dev., 15, 2973–3020, https://doi.org/10.5194/gmd-15-2973-2022, 2022.

Eyring, V., Bony, S., Meehl, G. A., Senior, C. A., Stevens, B., Stouffer, R. J., and Taylor, K. E.: Overview of the Coupled Model Intercomparison Project Phase 6 (CMIP6) experimental design and organization, Geosci. Model Dev., 9, 1937–1958, https://doi.org/10.5194/gmd-9-1937-2016, 2016.

Fetterer, F., Knowles, K., Meier, W. N., Savoie, M., Windnagel, A., and Stafford, T.: Sea Ice Index, Version 4, https://doi.org/10.7265/A98X-0F50, 2025.

Fogwill, C. J., Phipps, S. J., Turney, C. S. M., and Golledge, N. R.: Sensitivity of the Southern Ocean to enhanced regional Antarctic ice sheet meltwater input, Earth's Future, 3, 317–329, https://doi.org/10.1002/2015EF000306, 2015.

Gorte, T., Lovenduski, N. S., Nissen, C., and Lenaerts, J. T. M.: Antarctic Ice Sheet Freshwater Discharge Drives Substantial Southern Ocean Changes Over the 21st Century, Geophys. Res. Lett., 50, e2023GL104 949, https://doi.org/10.1029/2023GL104949, 2023.

Hattermann, T. and Levermann, A.: Response of Southern Ocean circulation to global warming may enhance basal ice shelf melting around Antarctica, Climate Dyn., 35, 741–756, https://doi.org/10.1007/s00382-009-0643-3, 2010.

Held, I. M., Guo, H., Adcroft, A., Dunne, J. P., Horowitz, L. W., Krasting, J., Shevliakova, E., Winton, M., Zhao, M., Bushuk, M., Wittenberg, A. T., Wyman, B., Xiang, B., Zhang, R., Anderson, W., Balaji, V., Donner, L., Dunne, K., Durachta, J., Gauthier, P. P. G., Ginoux, P., Golaz, J.-C., Griffies, S. M., Hallberg, R., Harris, L., Harrison, M., Hurlin, W., John, J., Lin, P., Lin, S.-J., Malyshev, S., Menzel, R., Milly, P. C. D., Ming, Y., Naik, V., Paynter, D., Paulot, F., Ramaswamy, V., Reichl, B., Robinson, T., Rosati, A., Seman, C., Silvers, L. G., Underwood, S., and Zadeh, N.: Structure and Performance of GFDL's CM4.0 Climate Model, J. Adv. Model. Earth Syst., 11, 3691–3727, https://doi.org/10.1029/2019MS001829, 2019.

Heuzé, C.: Antarctic Bottom Water and North Atlantic Deep Water in CMIP6 models, Ocean Science, 17, 59–90, https://doi.org/10.5194/os-17-59-2021, 2021.

Kaufman, Z., Wilson, E., Purich, A., Beadling, R., and Li, Y.: The Impact of Underestimated Southern Ocean Freshening on Simulated Historical Sea Surface Temperature Trends, Geophys. Res. Lett., 52, e2024GL112639, https://doi.org/10.1029/2024GL112639, 2025.

Kelley, M., Schmidt, G. A., Nazarenko, L. S., Bauer, S. E., Ruedy, R., Russell, G. L., Ackerman, A. S., Aleinov, I., Bauer, M., Bleck, R., Canuto, V., Cesana, G., Cheng, Y., Clune, T. L., Cook, B. I., Cruz, C. A., Del Genio, A. D., Elsaesser, G. S., Faluvegi, G., Kiang, N. Y., Kim, D., Lacis, A. A., Leboissetier, A., LeGrande, A. N., Lo, K. K., Marshall, J., Matthews, E. E., McDermid, S., Mezuman, K., Miller, R. L., Murray, L. T., Oinas, V., Orbe, C., García-Pando, C. P., Perlwitz, J. P., Puma, M. J., Rind, D., Romanou, A., Shindell, D. T., Sun, S., Tausnev, N., Tsigaridis, K., Tselioudis, G., Weng, E., Wu, J., and Yao, M.-S.: GISS-E2.1: Configurations and Climatology, J. Adv. Model. Earth Syst., 12, e2019MS002 025, https://doi.org/10.1029/2019MS002025, 2020.

Kuhlbrodt, T., Jones, C. G., Sellar, A., Storkey, D., Blockley, E., Stringer, M., Hill, R., Graham, T., Ridley, J., Blaker, A., Calvert, D., Copsey, D., Ellis, R., Hewitt, H., Hyder, P., Ineson, S., Mulcahy, J., Siahaan, A., and Walton, J.: The Low-Resolution Version of HadGEM3 GC3.1: Development and Evaluation for Global Climate, J. Adv. Model. Earth Syst., 10, 2865–2888, https://doi.org/10.1029/2018MS001370, 2018.

Mackie, S., Smith, I. J., Ridley, J. K., Stevens, D. P., and Langhorne, P. J.: Climate Response to Increasing Antarctic Iceberg and Ice Shelf Melt, J. Climate, 33, 8917–8938, https://doi.org/10.1175/JCLI-D-19-0881.1, 2020a.

Mackie, S., Smith, I. J., Stevens, D. P., Ridley, J. K., and Langhorne, P. J.: Interactions between Increasing CO2 and Antarctic Melt Rates, J. Climate, 33, 8939–8956, https://doi.org/10.1175/JCLI-D-19-0882.1, 2020b.

Matthes, K., Biastoch, A., Wahl, S., Harlaß, J., Martin, T., Brücher, T., Drews, A., Ehlert, D., Getzlaff, K., Krüger, F., Rath, W., Scheinert, M., Schwarzkopf, F. U., Bayr, T., Schmidt, H., and Park, W.: The Flexible Ocean and Climate Infrastructure version 1 (FOCI1): mean state and variability, Geosci. Model Dev., 13, 2533–2568, https://doi.org/10.5194/gmd-13-2533-2020, 2020.

Merino, N., Jourdain, N. C., Le Sommer, J., Goosse, H., Mathiot, P., and Durand, G.: Impact of increasing antarctic glacial freshwater release on regional sea-ice cover in the Southern Ocean, Ocean Model., 121, 76–89, https://doi.org/10.1016/j.ocemod.2017.11.009, 2018.

Muilwijk, M., Hattermann, T., Beadling, R. L., Swart, N. C., Nummelin, A., Guo, C., Chandler, D. M., Langebroek, P., Zhou, S., Dutrieux, P., Chen, J.-J., Danek, C., England, M. H., Griffies, S. M., Haumann, F. A., Jüling, A., Jouet, O., Li, Q., Martin, T., Marshall, J., Pauling, A. G., Purich, A., Song, Z., Smith, I. J., Thomas, M., Trombini, I., van der Linden, E., and Xu, X.: Large Regional Differences in Antarctic Ice Shelf Mass Loss from Southern Ocean Warming and Meltwater Feedbacks, EGUsphere, pp. 1–39, https://doi.org/10.5194/egusphere-2025-3747, 2025.

Parkinson, C. L.: A 40-y record reveals gradual Antarctic sea ice increases followed by decreases at rates far exceeding the rates seen in the Arctic, Proc. Natl. Acad. Sci. (USA), 116, 14 414–14 423, https://doi.org/10.1073/pnas.1906556116, 2019.

Pauling, A. G.: andrewpauling/sofiaice_tier1: sofiaice_tier1 v1.0 [Software], https://doi.org/10.5281/zenodo.18476161, 2026.

Pauling, A. G., Bitz, C. M., Smith, I. J., and Langhorne, P. J.: The Response of the Southern Ocean and Antarctic Sea Ice to Freshwater from Ice Shelves in an Earth System Model, J. Climate, 29, 1655–1672, https://doi.org/10.1175/JCLI-D-15-0501.1, 2016.

Pauling, A. G., Smith, I. J., Langhorne, P. J., and Bitz, C. M.: Time-Dependent Freshwater Input From Ice Shelves: Impacts on Antarctic Sea Ice and the Southern Ocean in an Earth System Model, Geophys. Res. Lett., 44, 10 454–10 461, https://doi.org/10.1002/2017GL075017, 2017.

Purich, A. and England, M. H.: Projected Impacts of Antarctic Meltwater Anomalies over the Twenty-First Century, J. Climate, 36, 2703–2719, https://doi.org/10.1175/JCLI-D-22-0457.1, 2023.

Rignot, E., Mouginot, J., Scheuchl, B., van den Broeke, M., van Wessem, M. J., and Morlighem, M.: Four decades of Antarctic Ice Sheet mass balance from 1979-2017, Proc. Natl. Acad. Sci. (USA), 116, 1095–1103, https://doi.org/10.1073/pnas.1812883116, 2019.

Roach, L. A. and Meier, W. N.: Sea ice in 2023, Nat. Rev. Earth Environ., 5, 235–237, https://doi.org/10.1038/s43017-024-00542-0, 2024.

Roach, L. A., Dörr, J., Holmes, C. R., Massonnet, F., Blockley, E. W., Notz, D., Rackow, T., Raphael, M. N., O'Farrell, S. P., Bailey, D. A., and Bitz, C. M.: Antarctic Sea Ice Area in CMIP6, Geophys. Res. Lett., 47, e2019GL086 729, https://doi.org/10.1029/2019GL086729, 2020.

Roach, L. A., Mankoff, K. D., Romanou, A., Blanchard-Wrigglesworth, E., Haine, T. W. N., and Schmidt, G. A.: Winds and Meltwater Together Lead to Southern Ocean Surface Cooling and Sea Ice Expansion, Geophys. Res. Lett., 50, e2023GL105 948, https://doi.org/10.1029/2023GL105948, 2023.

Schmidt, G. A., Romanou, A., Roach, L. A., Mankoff, K. D., Li, Q., Rye, C. D., Kelley, M., Marshall, J. C., and Busecke, J. J. M.: Anomalous Meltwater From Ice Sheets and Ice Shelves Is a Historical Forcing, Geophys. Res. Lett., 50, e2023GL106 530, https://doi.org/10.1029/2023GL106530, 2023.

Seland, Ø., Bentsen, M., Olivié, D., Toniazzo, T., Gjermundsen, A., Graff, L. S., Debernard, J. B., Gupta, A. K., He, Y.-C., Kirkevåg, A., Schwinger, J., Tjiputra, J., Aas, K. S., Bethke, I., Fan, Y., Griesfeller, J., Grini, A., Guo, C., Ilicak, M., Karset, I. H. H., Landgren, O., Liakka, J., Moseid, K. O., Nummelin, A., Spensberger, C., Tang, H., Zhang, Z., Heinze, C., Iversen, T., and Schulz, M.: Overview of the Norwegian Earth System Model (NorESM2) and key climate response of CMIP6 DECK, historical, and scenario simulations, Geosci. Model Dev., 13, 6165–6200, https://doi.org/10.5194/gmd-13-6165-2020, 2020.

Semmler, T., Danilov, S., Gierz, P., Goessling, H. F., Hegewald, J., Hinrichs, C., Koldunov, N., Khosravi, N., Mu, L., Rackow, T., Sein, D. V., Sidorenko, D., Wang, Q., and Jung, T.: Simulations for CMIP6 With the AWI Climate Model AWI-CM-1-1, J. Adv. Model. Earth Syst., 12, e2019MS002 009, https://doi.org/10.1029/2019MS002009, 2020.

Seroussi, H., Nowicki, S., Payne, A. J., Goelzer, H., Lipscomb, W. H., Abe-Ouchi, A., Agosta, C., Albrecht, T., Asay-Davis, X., Barthel, A., Calov, R., Cullather, R., Dumas, C., Galton-Fenzi, B. K., Gladstone, R., Golledge, N. R., Gregory, J. M., Greve, R., Hattermann, T., Hoffman, M. J., Humbert, A., Huybrechts, P., Jourdain, N. C., Kleiner, T., Larour, E., Leguy, G. R., Lowry, D. P., Little, C. M., Morlighem, M., Pattyn, F., Pelle, T., Price, S. F., Quiquet, A., Reese, R., Schlegel, N.-J., Shepherd, A., Simon, E., Smith, R. S., Straneo, F., Sun, S., Trusel, L. D., Van Breedam, J., van de Wal, R. S. W., Winkelmann, R., Zhao, C., Zhang, T., and Zwinger, T.: ISMIP6 Antarctica: a multi-model ensemble of the Antarctic ice sheet evolution over the 21st century, The Cryosphere, 14, 3033–3070, https://doi.org/10.5194/tc-14-3033-2020, 2020.

Sgubin, G., Swingedouw, D., Drijfhout, S., Mary, Y., and Bennabi, A.: Abrupt cooling over the North Atlantic in modern climate models, Nat. Commun., 8, 14 375, https://doi.org/10.1038/ncomms14375, 2017.

Shepherd, A., Ivins, E., Rignot, E., Smith, B., van den Broeke, M., Velicogna, I., Whitehouse, P., Briggs, K., Joughin, I., Krinner, G., Nowicki, S., Payne, T., Scambos, T., Schlegel, N., A, G., Agosta, C., Ahlstrøm, A., Babonis, G., Barletta, V., Blazquez, A., Bonin, J., Csatho, B., Cullather, R., Felikson, D., Fettweis, X., Forsberg, R., Gallee, H., Gardner, A., Gilbert, L., Groh, A., Gunter, B., Hanna, E., Harig, C., Helm, V., Horvath, A., Horwath, M., Khan, S., Kjeldsen, K. K., Konrad, H., Langen, P., Lecavalier, B., Loomis, B., Luthcke, S., McMillan, M., Melini, D., Mernild, S., Mohajerani, Y., Moore, P., Mouginot, J., Moyano, G., Muir, A., Nagler, T., Nield, G., Nilsson, J., Noel, B., Otosaka, I., Pattle, M. E., Peltier, W. R., Pie, N., Rietbroek, R., Rott, H., Sandberg-Sørensen, L., Sasgen, I., Save, H., Scheuchl, B., Schrama, E., Schröder, L., Seo, K.-W., Simonsen, S., Slater, T., Spada, G., Sutterley, T., Talpe, M., Tarasov, L., van de Berg, W. J., van der Wal, W., van Wessem, M., Vishwakarma, B. D., Wiese, D., Wouters, B., and The IMBIE team: Mass balance of the Antarctic Ice Sheet from 1992 to 2017, Nature, 558, 219–222, https://doi.org/10.1038/s41586-018-0179-y, 2018.

Siahaan, A., Smith, R. S., Holland, P. R., Jenkins, A., Gregory, J. M., Lee, V., Mathiot, P., Payne, A. J., Ridley, J. K., and Jones, C. G.: The Antarctic contribution to 21st-century sea-level rise predicted by the UK Earth System Model with an interactive ice sheet, The Cryosphere, 16, 4053–4086, https://doi.org/10.5194/tc-16-4053-2022, 2022.

Slater, T., Lawrence, I. R., Otosaka, I. N., Shepherd, A., Gourmelen, N., Jakob, L., Tepes, P., Gilbert, L., and Nienow, P.: Review article: Earth's ice imbalance, The Cryosphere, 15, 233–246, https://doi.org/10.5194/tc-15-233-2021, 2021.

Stroeve, J. and Notz, D.: Changing state of Arctic sea ice across all seasons, Environ. Res. Lett, 13, 103 001, https://doi.org/10.1088/1748-9326/aade56, 2018.

Swart, N. C. and Fyfe, J. C.: The influence of recent Antarctic ice sheet retreat on simulated sea ice area trends, Geophys. Res. Lett., 40, 4328–4332, https://doi.org/10.1002/grl.50820, 2013.

Swart, N. C., Cole, J. N. S., Kharin, V. V., Lazare, M., Scinocca, J. F., Gillett, N. P., Anstey, J., Arora, V., Christian, J. R., Hanna, S., Jiao, Y., Lee, W. G., Majaess, F., Saenko, O. A., Seiler, C., Seinen, C., Shao, A., Sigmond, M., Solheim, L., von Salzen, K., Yang, D., and Winter, B.: The Canadian Earth System Model version 5 (CanESM5.0.3), Geosci. Model Dev., 12, 4823–4873, https://doi.org/10.5194/gmd-12-4823-2019, 2019.

Swart, N. C., Martin, T., Beadling, R., Chen, J.-J., Danek, C., England, M. H., Farneti, R., Griffies, S. M., Hattermann, T., Hauck, J., Haumann, F. A., Jüling, A., Li, Q., Marshall, J., Muilwijk, M., Pauling, A. G., Purich, A., Smith, I. J., and Thomas, M.: The Southern Ocean Freshwater Input from Antarctica (SOFIA) Initiative: scientific objectives and experimental design, Geosci. Model Dev., 16, 7289–7309, https://doi.org/10.5194/gmd-16-7289-2023, 2023.

Swingedouw, D., Fichefet, T., Huybrechts, P., Goosse, H., Driesschaert, E., and Loutre, M.-F.: Antarctic ice-sheet melting provides negative feedbacks on future climate warming, Geophys. Res. Lett., 35, L17705, https://doi.org/10.1029/2008GL034410, 2008.

Thomas, M., Ridley, J. K., Smith, I. J., Stevens, D. P., Holland, P. R., and Mackie, S.: Future Response of Antarctic Continental Shelf Temperatures to Ice Shelf Basal Melting and Calving, Geophys. Res. Lett., 50, e2022GL102 101, https://doi.org/10.1029/2022GL102101, 2023.

Wang, C. and Beckmann, A.: Investigation of the impact of Antarctic ice-shelf melting in a global ice–ocean model (ORCA2-LIM), Ann. Glaciol., 46, 78–82, https://doi.org/10.3189/172756407782871602, 2007.

Weiffenbach, J. E., Dijkstra, H. A., von der Heydt, A. S., Abe-Ouchi, A., Chan, W.-L., Chandan, D., Feng, R., Haywood, A. M., Hunter, S. J., Li, X., Otto-Bliesner, B. L., Peltier, W. R., Stepanek, C., Tan, N., Tindall, J. C., and Zhang, Z.: Highly stratified mid-Pliocene Southern Ocean in PlioMIP2, Clim. Past, 20, 1067–1086, https://doi.org/10.5194/cp-20-1067-2024, 2024.

Xu, X., Martin, T., Beadling, R. L., Liu, J., Bischof, S., Hattermann, T., Huo, W., Li, Q., Marshall, J. C., Muilwijk, M., Pauling, A. G., Purich, A., Smith, I. J., Swart, N. C., and Thomas, M.: Robustness and Mechanisms of the Atmospheric Response Over the Southern Ocean to Idealized Freshwater Input Around Antarctica, Geophys. Res. Lett., 52, e2024GL113 734, https://doi.org/10.1029/2024GL113734, 2025.

Ziehn, T., Chamberlain, M. A., Law, R. M., Lenton, A., Bodman, R. W., Dix, M., Stevens, L., Wang, Y.-P., Srbinovsky, J., Ziehn, T., Chamberlain, M. A., Law, R. M., Lenton, A., Bodman, R. W., Dix, M., Stevens, L., Wang, Y.-P., and Srbinovsky, J.: The Australian Earth System Model: ACCESS-ESM1.5, Journal of Southern Hemisphere Earth System Science, 70, 193–214, https://doi.org/10.1071/ES19035, 2020.